



Published in final edited form as:

Nat Rev Chem. 2019 June ; 3(6): 375–392. doi:10.1038/s41570-019-0103-5.

Controlling the optical properties of carbon nanotubes with organic colour-centre quantum defects

Alexandra H. Brozena¹, Mijin Kim¹, Lyndsey R. Powell¹, YuHuang Wang^{1,2,*}

¹Department of Chemistry and Biochemistry, University of Maryland, College Park, MD, USA.

²Maryland NanoCenter, University of Maryland, College Park, MD, USA.

Abstract

Previously unwelcome, defects are emerging as a new frontier of research, providing a molecular focal point to study the coupling of electrons, excitons, phonons and spin in low-dimensional materials. This opportunity is particularly intriguing in semiconducting single-walled carbon nanotubes, in which covalently bonding organic functional groups to the sp^2 carbon lattice can produce tunable sp^3 quantum defects that fluoresce brightly in the shortwave IR, emitting pure single photons at room temperature. These novel physical properties have made such synthetic defects, or ‘organic colour centres’, exciting new systems for chemistry, physics, materials science, engineering and quantum technologies. This Review examines progress in this emerging field and presents a unified description of this new family of quantum emitters, as well as providing an outlook of the rapidly expanding research and applications of synthetic defects.

A defect in an otherwise perfect crystal is a singularity from which new chemistry and physics may arise. This prospect is particularly intriguing in low-dimensional crystals, such as single-walled carbon nanotubes (SWCNTs), because the defect site provides a focal point for electrons, excitons, phonons and spin to couple, fundamentally altering the collective electrical, optical, mechanical and thermal properties of the material. While the intrinsic properties of many low-dimensional crystals have been extensively studied in recent decades, to the point of being well understood^{1–6}, we are only beginning to appreciate how defects can constructively impact the chemical and physical properties of the host crystals.

This Review focuses on progress at the emerging frontier of fluorescent chemical defects that are synthetically created in semiconducting SWCNT hosts by covalently bonding organic molecules to the crystal lattice (FIG. 1). The defect produces a finite potential well within the extended sp^2 carbon lattice of the semiconductor host. Unlike native defects, which normally act as quenching traps for excitons, the transitions between the electronic states of these synthetic defects are allowed, producing photoluminescence that is unexpectedly bright⁷, chemically tunable^{7,8} and single photon in nature⁹. In the quickly

* yhw@umd.edu.

Author contributions

Y.H.W. conceptualized the work. A.H.B., M.K., L.R.P. and Y.H.W. jointly wrote the manuscript.

Competing interests

The authors declare no competing interests.

expanding literature, these defect centres have also been called sp^3 defects^{7,9-16}, molecularly tunable fluorescent quantum defects, fluorescent quantum defects, sp^3 quantum defects or simply quantum defects^{8,17}. In this Review, we adopt the term organic colour centres (OCCs), coined by Zheng and Srinivasan¹⁸, in reference to Wang and colleagues' introduction of this defect type and its molecular tunability⁷. When appropriate, we may also emphasize the quantum nature and geometry of these structures by referring to them as sp^3 quantum defects, or quantum defects for short. However, this should not be confused with the quantum defect that Schrödinger proposed in 1921 to describe a separate phenomenon regarding the deviation of the Rydberg formula¹⁹.

Because OCCs can be chemically tailored and experimentally probed at the single-defect level using spectroscopic methods, this novel synthetic quantum system has opened up exciting opportunities to determine the chemical nature of native defects in low-dimensional solids^{7,15,20-28}, explore new material properties^{8,16}, break the dark exciton limit of SWCNT fluorescence^{7,8}, promote upconversion photoluminescence^{29,30}, engineer quantum light sources^{9,18} and probe chemical events that may be otherwise difficult to capture¹². This field is also driven by the development of new experimental and theoretical approaches^{16,23,26,31} that have made it possible to study electron scattering^{32,33}, phonon coupling^{7,13,34}, exciton diffusion and trapping^{11,13,14,35-46}, and spin-orbit coupling⁴⁷ at chemically tailored defect sites, even at the single-defect limit⁴⁸, on carbon nanomaterials and other low-dimensional substrates, thus greatly expanding our understanding of the impact of defects. The unique combination of these properties and the possibilities that they suggest further distinguish OCC-based defects from other solid-state quantum systems, such as nitrogen-vacancy centres in diamond⁴⁹⁻⁵¹, quantum dots⁵²⁻⁵⁴ and carbon antisite-vacancy pairs in 4H-SiC (REF.⁵⁵), which are generally more limited in terms of molecular and host tunability, excitation and emission ranges, and quantum properties, such as room-temperature emission of high-purity single photons (TABLE 1).

In this Review, we discuss the creation and characterization of OCCs, as well as their theoretical characterization based on molecular dynamics and quantum mechanics simulations. We particularly focus on the effects of OCCs on the host substrate's electronic structure and optical properties. We also discuss the emergent applications of OCCs in chemical sensing, bioimaging, quantum information and several optoelectronic applications that require bright, high-quality quantum-light sources, including single-photon emitters. Although researchers are beginning to explore defects in various low-dimensional materials, such as 2D transition metal dichalcogenides (TMDs)^{20,27,56}, we initiate this discussion primarily within the context of SWCNTs, for which the physicochemical understanding of OCCs already has a strong foundation^{7,8,17,23,24,28,31,57-59}. However, we believe that this concept of fluorescent quantum defects can also be extended to other semiconductors, including those that are not themselves organic.

Following this brief introduction, we define the physical and chemical properties that make OCCs unique, focusing on their interplay with the exciton dynamics in SWCNTs, followed by a discussion of how OCCs can be created by covalently bonding functional groups to the nanotube crystal lattice. We then discuss emerging applications of OCCs and conclude with an outlook on new frontiers of OCCs in chemistry, physics, materials science and

engineering, as well as various potential applications of these unique, molecularly tunable quantum systems.

Single-walled carbon nanotubes

Defect-free SWCNTs.

For centuries, the uninterrupted and regular atomic structure of crystals and the physicochemical properties that arise from it have been extensively studied. Diamonds are an example of a near-perfect crystal, featuring a continuous, repeating lattice of sp^3 -hybridized carbon atoms. Silicon is another material in which its single-crystalline structure and atomic doping have been important for various high-impact, semiconductor-based applications, such as field-effect transistors and solar cells. Similarly, SWCNTs may be viewed as nanoscale carbon crystals made of graphene conceptually rolled up along a chiral vector that defines the nanotube's physical and electronic structure¹.

In semiconducting crystals, electrons, phonons and excitons are delocalized over an extended network or a continuum band of states, which manifest as electrical, thermal and optical transport properties. SWCNTs feature extended π -bond conjugation arising from the rigid sp^2 C–C bonds that give rise to an unusual combination of all three transport properties^{1,60,61}, including extraordinarily high carrier mobility ($>100,000 \text{ cm}^2 \text{ V}^{-1} \text{ s}^{-1}$) in semiconducting nanotubes⁶², room-temperature ballistic electron conductivity⁶³ and high thermal conductivity ($>2,000 \text{ W m}^{-1} \text{ K}^{-1}$, comparable to that of diamond) for metallic nanotubes^{64,65}. The nanotube crystal also demonstrates an exciton diffusion length as high as $\sim 550 \text{ nm}$ (REF.⁶⁶).

The 1D structure of SWCNTs results in distinct density of states featuring Van Hove singularities, the position of which depends on the nanotube roll-up vector, or chirality. The roll-up vector is defined by two structural indexes (n,m) that dictate the nanotube structure and its unique electronic band structure and bandgap¹. The absorption of light in the UV-visible (UV-vis) range corresponding to Van Hove transitions E_{33} and E_{22} results in the generation of a mobile exciton, which rapidly decays ($\sim 40 \text{ fs}$) to the lower-lying E_{11} excited state and potentially radiatively recombines in the near-IR (NIR; $\sim 800\text{--}1,600 \text{ nm}$)⁶⁷. The binding energies of nanotube excitons are on the order of several hundred millielectronvolts, making them effectively quasi-particles⁶⁸. In this regard, the way in which excitons interact with defects determines the various phenomena that arise from OCCs.

Quantum theory predicts that SWCNT excitons are composed of 4 singlet and 12 triplet excitonic states due to the spin degeneracy⁶⁹ and intervalley Coulombic interactions between the electron and the hole⁷⁰. Within the manifold of excitonic states, only one transition from the singlet state is optically allowed, the energy level of which is higher than the majority of the singlet or triplet dark states^{69,70}. Because of this, the bright exciton readily decays into the lower-lying dark singlet or triplet states^{71–73}, from which the excitation energy is typically lost as heat, contributing to the low photoluminescence quantum yields of SWCNTs⁷⁴ (FIG. 2a). The excitons diffuse along the SWCNT until they recombine; therefore, the optical and electronic transport properties of SWCNTs respond sensitively to the conditions surrounding them (including temperature and pH)^{66,75}. However, how these

properties are affected and even completely transformed by OCCs has only recently come into focus. Consequently, the ability to control the fate of excitons and OCCs in crystals is crucial for employment in photovoltaics, lighting, imaging, sensing and other important optoelectronic applications.

Defects in SWCNTs.

Defects, including substitutions, vacancies, dangling bonds and step edges, are known to have a significant impact on a crystal's physical properties⁷⁶. For example, nitrogen vacancies in diamond are known for stable, room-temperature, single-photon emission, which is advantageous for quantum information processing⁵¹. For SWCNTs, scanning probe and electron microscopy studies have revealed that these materials are rarely, if ever, perfect crystals. Some degree of structural defects always exists, such as oxygenated and dangling bonds at the nanotube ends, carbon vacancies, sp^3 point defects and/or rotated bonds (such as Stone–Wales defects)^{48,77–79}. Using an electrochemical technique, Collins and co-workers⁴⁸ determined that the defect density can be as low as one in every 4 μm of high-quality, chemical-vapour-deposition-grown SWCNTs. However, additional defects may become implanted during chemical processing for subsequent applications, which is one of the several hypothesized reasons for the low photoluminescence quantum yields of SWCNTs, as extensive degradation of the graphitic structure is known to readily quench mobile excitons before they can radiatively decay^{75,78,80–82}. We will not be commenting on these types of defects or their resulting impacts at different dimensional regimes, as there are already excellent reviews that cover these subjects^{83–85}. Rather, we focus on OCCs, which can be synthetically created in SWCNTs and provide more chemically defined systems for quantitative characterization than native defects.

OCCs feature four defining characteristics

First, OCCs are quantum, two-level systems incorporated within the host semiconductor. Second, OCCs trap and localize excitons, increasing the probability of radiative recombination, as well as enabling single-photon emission. Third, the presence of OCCs on SWCNTs leads to bright photoemissions, as they induce the formation of optically bright excitonic states that lie below dark excitons. Last, OCCs are chemically tunable, an important defining characteristic that is discussed in detail in the following sections.

OCCs are quantum, two-level systems.

Normally, defects are thought to impede electronic transport in semiconductors, acting as scattering centres for electrons and holes and quenching traps for excitons^{48,75,80}. However, the addition of an organic functional group to a SWCNT by means of symmetry-breaking covalent functionalization can generate a new two-level state (associated with a new possible optical transition, E_{11}^-) localized within the continuum bands of the semiconducting host (for simplicity, here, we use E_{ij} in reference to both the optical transition and the energy of the transition, as well as the states associated with it; FIG. 2a). Thus, mobile E_{11} excitons can be channelled to and trapped in this new lower-energy state, producing a new emission that is redshifted from the native E_{11} fluorescence. In this manner, the electronic and

chemical nature of a single defect can profoundly change the photophysical properties of the substrate.

The hypothesis above was experimentally verified by demonstrating that the covalent addition of aryl groups to the SWCNT surface results in the generation of a potential well in the nanotube's electronic structure⁷. This modification leads to the appearance of an E_{11}^- emission band in the spectrum of 4-nitrobenzene-functionalized (6,5)-SWCNTs that is redshifted with respect to the E_{11} emission corresponding to the pristine SWCNT⁷ (FIG. 2b). Note that this new photoluminescence peak is observed at a relatively low functionalization density. With the excessive addition of defects to the nanotube, the E_{11}^- fluorescence eventually fades owing to the loss of the sp^2 -conjugated structure, preventing photoexcitation at the E_{11} transition. Density functional theory (DFT) calculations suggest that this dipole-allowed transition is a result of an asymmetric splitting (by 105–326 meV) of the frontier orbitals of the SWCNT host at the induced sp^3 defect⁷. This orbital splitting effectively creates a localized, two-level system within the otherwise continuous bands of the nanotube host. The energy levels of this two-level system can be tuned by incorporating electron-withdrawing or electron-donating moieties in the aryl group, which adjust the HOMO and LUMO levels of the OCC-induced defect states⁷.

The ability to chemically tune the energy levels of OCCs can be greatly enhanced by using aqueous alkyl halide-based reactions that enable virtually any bromine-containing or iodine-containing hydrocarbon precursor to be covalently attached to the nanotube surface⁸. In this way, the nature of the defect and the consequent induced emission can be readily tuned based on the inductive electronic effects of the covalently attached functional group, which can be predictively estimated by calculating the group's Taft constant⁸. For instance, diiodide reactants can be used to generate divalent functional groups that are attached to the nanotube surface through cycloaddition. Such divalent defects induce a substantially more redshifted emission than their monovalent counterparts (132 meV versus 163 meV for (6,5)-SWCNT-CH₃ and (6,5)-SWCNT>CH₂, respectively). The presence of fluorine atoms on the alkyl chain further increases the redshift of the resulting E_{11}^- peak (132 meV and 194 meV for (6,5)-SWCNT-CH₃ and (6,5)-SWCNT-CF₃, respectively)⁸.

Two-level systems inherently emit single photons⁸⁶. This quantum feature of OCCs was initially proposed as speculation⁷ and recently experimentally confirmed through photon antibunching measurements, revealing that OCCs are indeed bright, room-temperature, single-photon emitters⁹. High-purity (99%) single-photon emission of the E_{11}^- peak was observed by functionalizing SWCNTs of three different chiralities — (6,5), (7,5) and (10,3) — with two different diazonium agents (4-methoxybenzenediazonium and 3,5-dichlorobenzenediazonium). In this case, the E_{11}^- emission ranged between 1,100 nm and 1,600 nm, which effectively covers the O and C bands of telecom wavelengths utilized in fibre-optic communications⁹. Importantly, the emissions were observed at room temperature and were also stable at high excitation pumping power, demonstrating high single-photon count rates ($>10^5$ s⁻¹, with the possibility to approach 10–100 MHz). Thus, engineering both the functional group and the semiconductor host (that is, the nanotube chirality and the corresponding bandgap) is important for highly tunable single-photon emission, the applications of which are discussed in later sections.

Strikingly, this two-level system features a new optical signature that can completely dominate that of the host. Although the absorption spectra are nearly unchanged, the photoluminescence is almost entirely shifted from E_{11} to the new defect-induced photoluminescence at E_{11}^- , as clearly shown in the spectra in FIG. 2b (REF.⁷). This phenomenon suggests that these OCC-tailored SWCNTs may be treated as new quantum systems that are distinctly different from their nanotube hosts.

OCCs trap and localize excitons.

Interestingly, the native and OCC-induced photoluminescence for a given nanotube chirality share the same excitation wavelength. As the intensity of the E_{11}^- defect peak increases, the quantum yield of the intrinsic E_{11} SWCNT emission decreases^{7,8} (FIG. 2b). This behaviour and the generation of a two-level state in the host semiconductor's electronic structure by the incorporation of an OCC suggests that mobile E_{11} excitons are channelled to the defect site, where radiative recombination can occur. This explains why low OCC densities in SWCNTs have a minimal effect on the absorption spectra of these materials, yet feature an unexpectedly large impact on the nanotube photoluminescence. This E_{11}^- radiative transition can dominate the emission spectrum with substantially enhanced quantum yield compared with the native E_{11} transition⁷ and can even be used to bypass self-quenching routes in highly concentrated nanotube solutions owing to the effective Stokes shift between the E_{11} absorption and the E_{11}^- emission⁸⁷. This photoluminescence brightening effect is discussed in greater detail in the next section. The trapping of excitons at OCC sites is also supported by the observation that the position and intensity of their induced emission strongly depends on the organic functional groups. The energy difference between E_{11} and E_{11}^- can be tuned by ~130–260 meV for a single-chirality SWCNT, such as (6,5)-SWCNT, depending on the functional group added, with greater redshifts occurring for more-electron-withdrawing groups^{7,8,28} (FIG. 3a).

Exciton trapping at OCCs can be more directly visualized as hot spots in photoluminescence mapping images. For example, Doorn and colleagues³⁶ studied oxygen, 4-methoxybenzene and 4-bromobenzene functional groups on SWCNTs using photoluminescence imaging to provide more direct evidence of the trapping of diffusive excitons at these defect sites (FIG. 3b). Photoluminescence from the E_{11} transition is nearly continuous over the length of the nanotube, whereas photoluminescence arising from the E_{11}^- transition is spatially localized, within the diffraction limit. The green and red emissions due to the E_{11} and E_{11}^- transitions, respectively, appear in complementary positions along the nanotube length, even though they share the same source of excitons. This is further evidence in support of the exciton diffusion and defect-trapping model and demonstrates that the E_{11}^- transition is not directly promoted by light in these experiments³⁶. The interrelated character of the E_{11} and E_{11}^- peaks is also supported by time-dependent DFT modelling, which shows that the combined oscillator strength of these states remains effectively constant both before and after functionalization, suggesting a redistribution of E_{11} excitons to the E_{11}^- state^{39,88}. Super-resolution imaging at a resolution of <25 nm, which is well below the diffraction limit, has unambiguously confirmed the localization of excitons at fluorescent OCCs¹⁶. Remarkably, these imaging experiments were performed on OCCs added to ultrashort SWCNTs (just ~40

nm in length), which are substantially shorter than the exciton diffusion length, demonstrating efficient trapping of excitons at such organic defects (FIG. 3c,d).

The trapping of E_{11} excitons at OCCs prevents them from descending into non-radiative pathways. Not only does exciton trapping at OCCs shorten the E_{11} photoluminescence lifetime¹⁴ but it also spatially localizes the mobile E_{11} excitons to the defect trap, which reduces their dimensionality from 1D to 0D. This is expected to enhance the quantum yield of defect-trapped excitons by increasing their radiative lifetime. First, localizing an exciton at an OCC will decrease its size, which can enhance the radiative decay rate of E_{11}^- excitons^{13,89,90}. Additionally, owing to the 1D nature of E_{11} SWCNT excitons, their radiative decay rates are limited by the momentum mismatch between photons and thermally excited excitons in the 1D band dispersion. This restriction is responsible for the characteristic 1D radiative decay rate that is proportional to $T^{-1/2}$. However, localized excitons are free from the momentum restriction, which could lead to an increased radiative decay rate⁹⁰⁻⁹².

Although E_{11}^- excitons can escape local defects by thermal detrapping, this process is inefficient at room temperature (less than 5% of trapped E_{11}^- excitons escape back to the E_{11} state for aryl-functionalized (6,5)-SWCNTs) owing to the deep trapping depth of the potential well¹³. Photoluminescence arising from OCCs also exhibits strong nonlinear behaviour with increasing power density, even far below the high-power regime ($\gg 1$ kW cm⁻²), at which efficient exciton–exciton annihilation of E_{11} excitons takes place⁹³. This behaviour is consistent with an efficient accumulation of photogenerated E_{11} excitons into the sparse local defects.

OCCs brighten dark excitons.

Covalent functionalization of SWCNTs was long believed to introduce defects that decrease the already low (~1%) photoluminescence quantum yield of the material^{75,80}. However, if the covalent chemistry is sufficiently controlled, through the chemical nature of the functional groups, their density and location along the nanotube axis and in relation to other functional groups (see Controlling OCC density section), the SWCNT fluorescence can, in fact, be brightened through the new E_{11}^- emission by as much as 28-fold⁷.

This brightening effect suggests that the OCC-induced energy level not only resides below the bright E_{11} Van Hove transition but also below the dark excitonic states that are ~5–100 meV lower than the bright excitonic levels, and which normally act as efficient non-radiative pathways^{71,94}. In this manner, exciton diffusion and trapping by these OCCs can efficiently populate the defect state, which is low-lying and intrinsically bright, allowing the previously inaccessible dark excitons to be harvested (FIG. 4a). In this sense, dark excitons, like bright ones, may migrate to an OCC site, become trapped at the quantum well and emit through this new, optically allowed state. The lifetimes of both the dark and the bright E_{11} excitons become progressively shorter with increasing density of OCCs, which suggests that both dark and bright E_{11} excitons can become trapped at the defect site¹⁴.

The E_{11}^- redshift shows a $1/d^2$ SWCNT diameter (d) dependence and also a chirality family pattern, in which the SWCNTs are grouped by $\text{mod}(n-m,3) = 1$ or 2 , with $\text{mod}(n-m,3) = 1$

located above the centre line and $\text{mod}(n-m,3) = 2$ below^{7,8} (FIG. 4a). These trends closely follow what was predicted for dark excitons^{70–73}. Furthermore, the difference in energy between E_{11} and E_{11}^- corresponds to the energy of the defect-induced D-phonon mode ($1,301 \text{ cm}^{-1}$; 161 meV), which indicates a possible exciton–phonon coupling mechanism that facilitates the brightening of dark excitons through the defect. The increase in photoluminescence quantum efficiency is also strongly dependent on the functional group used, as demonstrated by the linear correlation of the E_{11}^- energy shift (relative to E_{11}) with the Hammett constant of aryl-defect substituents^{7,95} (FIG. 4b). Therefore, electron-withdrawing or electron-donating substituents can be used to tune the position of the E_{11}^- peak, providing an opportunity to not only control the OCC emission wavelength but also its emission intensity through phonon coupling with the dark exciton states of the nanotube⁷. This exciton–phonon coupling at defect sites also leads to a substantial vibrational reorganization of the SWCNT around the site of the OCC upon exciton trapping¹³.

Oxygen dopants have also been shown to produce a redshifted emission reminiscent of the E_{11}^- peak^{38,90,96,97}; however, temperature-dependent photoluminescence studies suggest that a low-lying dark state exists below the optically allowed states of oxygen-defect-trapped excitons⁹⁰. This experimental observation is consistent with time-dependent DFT calculations, which suggest that the oxygen-induced excitonic state is intrinsically dark, with its optically allowed state lying above the lowest energy level of the trapped exciton¹³. Although more studies are needed to elucidate this important characteristic, the dark excitonic states induced by oxygen defects ultimately limit the photoluminescence quantum yield. Oxygen dopants also lack the molecular tunability of OCCs, which provides multifaceted potential for these synthetic defects.

OCCs are molecularly tunable

From the chemical perspective, a remarkable feature of OCCs is that nearly any organic functional group has the potential to generate these unique colour centres in SWCNTs. However, to be photoluminescent, the defect must also generate a localized electronic state that is optically allowed. At present, only a few chemical reactions have been experimentally demonstrated to produce OCCs on SWCNTs, including those based on the propagative Billups–Birch reaction^{98,99}, aryl diazonium salts^{7,9,14,23,36,57}, diazoethers⁵⁸, and alkyl and aryl halides^{8,17} (FIG. 5). However, we anticipate that many more will soon be discovered, particularly as the chemical and physical nature of these defects becomes clearer.

As low functional group densities are typically required to create OCCs, they are somewhat difficult to probe by traditional methods, such as Raman spectroscopy and UV–vis–NIR absorption, because the crystal's overall electronic structure tends to dominate the spectra, making it difficult to observe the minority transitions. However, the shortwave IR photoluminescence of OCCs is redshifted and bright enough to be resolved from that of the native crystal. As a result, various photoluminescence spectroscopy techniques are convenient methods for monitoring the formation of defects in situ as the reaction proceeds, making it possible to tailor and optimize the chemistry and crystal hosts, as well as establish unambiguous structure–property relationships for these fluorescent defects. What follows is a discussion of the various chemical approaches that have been used to create OCCs on

SWCNTs and how researchers have taken advantage of the resulting defect-induced photoluminescence as a sensitive optical fingerprint to measure the extent of reactions on these structures.

Billups–Birch reduction.

One of the first functionalization methods to result in the observation of OCCs was the Billups–Birch reduction, although it was not fully understood at the time^{98,99} (FIG. 5e). This reaction, which involves the solvation of electrons using sodium or lithium in liquid ammonia (approximately $-30\text{ }^{\circ}\text{C}$), is highly effective at disrupting the van der Waals attractive forces between nanotubes to generate individually dispersed materials. This formation of a nanotube suspension is a necessary step to expose SWCNT sidewalls to the reactants. Alkyl halide reactants can then be added to this solution to form radical intermediates upon electron transfer from the reduced SWCNTs, which then react with the nanotube sidewalls to form covalently attached functional groups. Before the observation of OCCs as a result of this reaction, mechanistic study and Mulliken population analysis suggested that charges tended to localize around existing or added defects⁹⁸. This drives subsequent functionalization to occur near these sites for a propagating reaction mechanism that results in the formation of bands of alkyl functional groups along the nano tube⁹⁸. This clustering leaves significant portions of the sp^2 carbon lattice intact, such that its relative signatures in both the absorption and photoluminescent spectra are retained (although somewhat attenuated) after functionalization.

Covalent functionalization by the Billups–Birch reduction was subsequently confirmed to generate E_{11}^- photoluminescence in the emission spectrum, in which the emission energy is weakly dependent on the chemical identity of the functional group⁹⁹. However, owing to the limitations of this reaction, only substituents featuring different terminal atoms were studied. Additionally, the bulk nature of this approach makes it difficult, although not impossible, to work with chirality-purified SWCNTs, which are typically suspended by surfactant in aqueous solutions and available in small quantities, making them inadequate for the Billups–Birch reaction. Regardless of these impediments, the Billups–Birch reduction was unambiguously demonstrated to generate OCCs⁹⁹.

Aryldiazonium salts.

Aryldiazonium salts, such as 4-chlorobenzenediazonium tetrafluoroborate, have been widely used to functionalize graphite, nanocarbon^{100,101}, graphene¹⁰² and other 2D materials¹⁰³. The mechanism behind this reaction involves rapid, non-covalent adsorption of the aryldiazonium molecule to the nanotube and a subsequent slower covalent bond addition that is initiated by electron transfer from the nanotube to the reactant to form a radical that initiates the formation of a C–C bond with the graphitic surface^{100,104,105}. Before the discovery of OCCs, this type of covalent modification was mistakenly thought to create chemical defects that quench the SWCNT photoluminescence^{75,106}.

However, it turns out that aryldiazonium salts can introduce OCCs to SWCNTs, as first shown by Wang and colleagues⁷. The reaction of SWCNTs with aryldiazonium salts at low defect density (<1 defect per 20-nm length) results in the appearance of a new defect-

induced emission peak (E_{11}^-), redshifted by up to 254 meV from the native nanotube fluorescence, and an enhancement of the quantum yield by as much as 28-fold on the ensemble level⁷ (FIG. 5a). Further molecular tunability can be achieved using bisdiazonium salts (FIG. 5d). In this case, the E_{11}^- redshift has been demonstrated to depend on the length of the methylene spacer between the aryldiazonium fragments, suggesting a strong effect of defect proximity or density on the electronic structure of the OCC-modified nanotube²³.

One of the common themes in carbon nanochemistry is the use of radical-initiated reactions to achieve the covalent addition of OCCs, most likely owing to the stable and somewhat inert character of the sp^2 carbon lattice. However, a stable intermediate in the radical-initiated reaction provides the opportunity to drive the reaction more selectively by photoexciting the nanotube to initiate functionalization with aryldiazonium salts. Interestingly, resonant optical excitation of the SWCNT markedly accelerates the normally slow aryldiazonium chemistry by 154-fold⁵⁷. A higher irradiation power density also increases the degree of functionalization, as monitored through the defect-induced E_{11}^- emission, which, in addition to thermal controls, suggests that the photoactivated reaction is primarily driven photothermally. However, wavelength-dependence studies indicate that electron transfer does occur to some degree, opening the door for chirality-selective functionalization within a mixture of SWCNT chiralities⁵⁷.

Optically driven diazoether reactions.

Chirality-selective functionalization of SWCNTs is difficult to achieve owing to the myriad of competing properties influencing the nanotube reactivity (such as diameter and electronic type). However, it has been shown that light can drive the isomerization of diazoether 3-*O-p*-nitrobenzenediazoascorbic acid (*p*-NO₂-DZE) to display chirality-selective reactivity towards targeted SWCNTs⁵⁸ (FIG. 5b). In a demonstrated example, (6,5)-SWCNTs are excited with 565-nm light, which corresponds to the SWCNT's E_{22} transition, to generate covalently bonded nitroaryl groups and strong E_{11}^- photoluminescence. Without exposure to light, the OCC photoluminescence was not observed. This optically driven reactivity derives from pH-dependent isomerization of the unreactive *E* isomer of *p*-NO₂-DZE to the reactive *Z* isomer by energy transfer from the photoexcited SWCNT.

When this reaction is performed in a 1:1 mixture of (6,5)-SWCNTs and (7,3)-SWCNTs, excitation with 565-nm light (corresponding to the E_{22} transition of the (6,5)-SWCNT) results in almost exclusive reaction of the (6,5) nanotubes. When the E_{22} transition of the (7,3)-SWCNT is excited by 505-nm light, the defect-induced photoluminescence is observed much more strongly for the (7,3) species, whereas the smaller diameter, and, therefore, more reactive, (6,5)-SWCNTs barely react. This chiral selectivity is unprecedented, and although the photoluminescence intensity of E_{11}^- has not yet been directly correlated with the absolute number of implanted defects, it does provide a useful tool for measuring the relative reactivity of different components in a complex mixture⁵⁸.

Alkyl and aryl halide chemistry.

Wang and colleagues⁸ have demonstrated the extent of molecular tunability possible for OCCs with the development of relatively simple reactions involving alkyl and aryl halides

(FIG. 5c,f). These reactions, involving just sodium dodecyl sulfate (SDS)-dispersed SWCNTs in aqueous solution, an alkyl or aryl iodide reactant, acetonitrile and the mild reducing agent sodium dithionite, have demonstrated the ability to covalently attach over 30 different functional groups to SWCNTs at room temperature. They can also be used to attach both monovalent and divalent moieties to the nanotube surface. With the diversity of functional groups available, the defect-induced E_{11}^- peak can be redshifted by as much as 200 meV from the native E_{11} emission in (6,5)-SWCNTs (TABLE 2), increasing the quantum yield by an order of magnitude⁸. The molecular tunability of these reactions is made possible by the flexible use of almost any iodide-containing (and a few bromide-containing or chloride-containing) hydrocarbon-based compounds. DFT calculations also suggest that, like the Billups–Birch reaction⁹⁸, functionalization is favoured near existing defects (specifically, the para-position), at which charges tend to accumulate according to Mulliken analysis⁸, suggesting the likelihood of propagative functionalization for banding or clustered defect structures.

In addition to the numerous functional groups that can be added with the alkyl halide chemistry, photoinduced functionalization of aryl halides can be achieved by exciting the host semiconductor nanotube with resonant light¹⁷. (6,5)-SWCNTs were excited with various wavelengths in the presence of 4-iodoaniline, which absorbs in the UV region. When mixtures of reactants were irradiated, the resulting ratio of the integrated areas of the E_{11}^- and E_{11} emission peaks (at 1,130 nm and 980 nm, respectively) increased most substantially for irradiation energies that corresponded to the E_{33} absorption wavelength. The lack of functionalization under excitation energies corresponding to E_{11} was posited to be a result of insufficient energy to overcome the reaction barrier. Notably, without irradiation, no functionalization was detected, even when the sample was heated to 70 °C, making it possible to drive this OCC chemistry selectively with light.

These observations suggest that these reactions follow a photochemical rather than a photothermal mechanism. Although more experiments are required to verify this hypothesis, the excitation of an electron from the host semiconductor's ground state to the conduction band may have resulted in subsequent electron transfer to the LUMO of physisorbed, halide-containing aryl groups and triggered the reaction¹⁷. This degree of reaction control using light suggests the potential for chirality-selective functionalization and lithographic patterning of OCCs.

Controlling OCC density.

Time-resolved fluorescence and photoluminescence imaging studies suggest that the average exciton diffusion length in SWCNTs is ~100–550 nm (REFS^{66,75,81,107}). As most nanotubes are only a few hundred nanometres in length, excessive functionalization — such that the average distance between defects is much shorter than the exciton diffusion length — may result in the total loss of E_{11} photoluminescence. Additionally, extensive conversion of sp^2 -hybridized carbon into sp^3 through covalent functionalization results in the loss of the Van Hove transitions, eventually preventing the nanotube from being optically excited. These scenarios were consistently observed for covalently functionalized SWCNTs for many years,

leading to the mistaken belief that the addition of any defects to the nanotube would quench fluorescence^{75,80}.

However, at low defect densities in which the SWCNT graphitic structure remains largely intact, thus retaining the E_{22} excitation transition, not only can part of the E_{11} photoluminescence intensity be preserved but also the high quantum yield of the OCC-induced E_{11}^- emission can become the new fluorescent signature of the nanotube. For this situation to occur, OCC functional groups must be either spatially isolated within the exciton diffusion length⁷ or clustered together in functional bands⁹⁸, in both cases effectively retaining part of the conjugated sp^2 crystal structure. This will allow the nanotube to absorb photons in addition to retaining its excitonic transport properties.

There are different strategies for controlling the OCC density. In the case of diazonium-based reactions, the concentration of the reactant may simply be limited to ensure that the nanotubes are not overly functionalized. At the ensemble level, approximately one defect per 20 nm of (6,5)-SWCNT length, corresponding to 0.05% of carbon atoms functionalized with aryl defects, results in the highest defect-induced emission intensity⁷. The use of sodium deoxycholate in place of SDS as the surfactant can physically protect the nanotube surface, which helps limit the number of accessible sites for diazonium molecules to react¹⁴. Notably, light-activated reactions can be an effective method for controlling the degree of functionalization and the resulting defect emission^{8,17,57}. Adding defects in a more spatially controlled manner, such as through clustering or banding using reactions that propagate from existing defects, can help to retain the fluorescent features of the nanotube by keeping sufficient portions of the native crystal intact and, thereby, creating an effectively low defect density, even when the number of functional groups added to the nanotube surface is relatively high^{98,99}.

Using light to generate patterns of OCCs on different surfaces and materials could open up opportunities for generating substrates that feature both chemical and optical functionalities. For example, aqueous suspended (6,5)-SWCNTs can be selectively functionalized with 4-iodoaniline using light that is absorbed by the substrate's Van Hove transitions, indicating that a photoelectron transfer mechanism is behind the addition of the aryl groups¹⁷. The added defects generate bright, shortwave IR E_{11}^- emission at 1,130 nm, which could be used for molecular-level patterning, optical cryptography (such as shortwave-IR inks for security and authentication purposes) and biosensing in pre-patterned microarray and nanoarray applications¹⁷. A unique aspect of this proposed photolithographic mechanism is the fact that the substrate itself fluoresces (that is, the SWCNT), as opposed to the bonding molecule, in which case, we can anticipate the possibility of creating spatially correlated OCCs.

Configuration effects of OCCs.

An OCC involves a pair of sp^3 defects or many functional groups that presumably cluster to collectively form a defect site on the SWCNT. One intriguing question is what relative positions the functional groups take on the sp^2 lattice and how the atomic configuration of the OCC may impact the properties of the colour centre and the host.

Several groups have observed that difunctionalized nanotubes, in which the chemical reaction simultaneously implants two functional groups on the substrate within close proximity to each other, exhibit E_{11}^- photoluminescence that is considerably more redshifted than the monofunctionalized counterparts. For example, dialkylation reactions involving butyl lithium and butyl bromide induce the appearance of an E_{11}^- peak that is shifted by ~ 270 meV from the native (6,5) emission²¹. Similarly, the addition of two proximal aryl functional groups on the surface of (6,5)-SWCNTs by means of bisdiazonium salts results in an E_{11}^- peak shift of ~ 270 meV (REF.²³), the position of which surprisingly coincides with the dialkylation case and is close to that of defect-trapped triions in the same nanotube host¹¹. By contrast, monovalent diazonium reagents tend to produce defect peak shifts of just ~ 180 meV in SWCNTs of the same chirality⁷. A similar effect is also observed for divalent OCCs, although to a lesser extent⁸. Interestingly, density-functional tight-binding calculations found that the large energy shifts may emanate from strong coupling in the two distanced bonding sites owing to strong resonance effects²³. DFT calculations and low-temperature photoluminescence spectroscopy show that, owing to the radical-based mechanism of diazonium addition, the covalent bonding of an aryl group and hydrogen atom to the nanotube surface is limited to six different configurations that correspond to the ortho-position and the para-position¹⁵. Furthermore, these six defect configurations have distinct emission spectra in the NIR that range from $\sim 1,000$ nm to 1,350 nm for (6,5)-SWCNTs.

These initial findings indicate that we must better understand the impact of the OCC configuration, as it has a clear effect on the emission properties that could be both an advantage in terms of tunability and also a detriment if we are unable to control it. The inability to precisely control the atomic configuration of OCCs may cause inhomogeneous broadening of the defect-induced photoluminescence or even multiple emission peaks²³. This will be particularly problematic for potential applications of OCCs that will require uniform, if not identical, emitters. The use of diazonium salts has demonstrated some configurational selectivity, with the tendency to functionalize ortho-site carbon atoms in zigzag SWCNTs, which results in a threefold narrowing of the defect-induced emission³¹. DFT calculations suggest that this observation could be explained by the high symmetry of zigzag nanotubes, which limits the possible atomic configurations of the OCCs.

Emergent applications of OCCs

Beyond learning about the fundamental effects of defects on low-dimensional materials, OCCs may also have important practical implications. OCCs induce substantially brighter emissions than the hosts themselves, an important step towards the application of these materials in areas such as imaging, sensing and optoelectronics^{9,12,18,24,29,108}, in which photon conversion efficiency is key. In contrast to conventional defects, OCCs provide beneficial new chemical and physical properties that may have transformational impacts on quantum information, energy and biomedical innovations.

Sensing.

Although the strong optical and electrical properties of SWCNTs have made them obvious choices for sensing applications, unfunctionalized SWCNTs generally cannot differentiate

between small molecular species, making it difficult to sense specific chemicals, such as H^+ , in the complex chemical environment of a biological system¹². This challenge may be addressed with OCCs that can be chemically tailored to create bioimaging probes and chemical sensors with ultrahigh sensitivity and selectivity. For the most part, such SWCNT-sensing mechanisms can be based on modifications to their electrical properties (as monitored using the nanotubes as the channel component of a field-effect transistor), but success has also been found by measuring changes to the fluorescence emissions of individually dispersed SWCNTs as they interact with the target analyte^{109,110}.

Defect-induced photoluminescence is extremely sensitive to the local microenvironment, as demonstrated by the shifting of the emission wavelength as a function of the electron-withdrawing nature of the functional group^{7,8}. This sensitivity can be capitalized on for sensing small molecules or even ions by taking advantage of changes to the defect's inductive effect upon binding to another species. For example, by adding phenylboronic acid functional groups on the sidewall of a (6,5)-SWCNT, the resulting E_{11}^- fluorescence substantially shifts when exposed to a saccharide²⁴. The molecular recognition between the boronic acid group on the phenyl ring and the saccharide modifies the inductive effect of the OCC, causing it to become a stronger electron donor upon bonding to these molecules. Additionally, the responsiveness of the E_{11}^- shift appears to depend on the saccharide (D-fructose or D-glucose), which was hypothesized to be due to the different binding constants of these molecules with the borate complex. These findings indicate the potential use of E_{11}^- peak shifts to sense the presence of targeted analytes through molecular recognition. Various non-covalent methods of functionalizing SWCNTs have been developed that enable biological molecules to be attached to the nanotube sidewalls^{110–113}. Establishing similar techniques using OCCs suggests a powerful strategy for biosensing applications, given the tissue transparency of the NIR E_{11}^- emission¹¹⁴. Shiraki and co-workers developed an approach for sensing transition metal cations based on azo-crown-ether-functionalized aryl groups covalently bound to (6,5)-SWCNTs²⁶. In this work, the group showed how the emission of the implanted OCC (1,134 nm) shifts by up to 161 nm (~136 meV) in response to the concentration of Ag^+ ions binding within the cavity of the crown ring.

OCCs have also demonstrated potential as a pH sensor¹². Using diazonium salts, Wang and colleagues covalently attached *N,N*-diethyl-4-aminobenzene to SWCNTs and produced a functioning, all-optical pH and temperature nanosensor (FIG. 6a,b). The covalent addition of this molecule to the nanotube surface induces the appearance of the E_{11}^- emission at 1,120 nm at a pH of 7.40. Lower pH solutions result in protonation of the amino group and a significant redshift of the E_{11}^- position, whereas the wavelength of E_{11}^- remains unaffected. In this manner, the position of E_{11}^- shifts as the pH changes from 4.5 to 8.5, which covers the physiological pH window (pH 5.5–8.0). The larger peak shift can be attributed to the greater difference in the Hammett constant between the protonated and unprotonated forms of the OCC, as this has a direct effect on the trapping depth of the E_{11}^- excitons. This sensing mechanism is chemically specific: only the OCCs that feature the amino group respond to H^+ ; other groups, such as benzene, do not cause any observable spectral shift. Additionally, the aminoaryl-functionalized SWCNTs can be used to monitor the temperature of the solution, as increased thermal energy enables defect-trapped excitons to escape the

potential well, diminishing the integrated intensity ratio of $E_{11}^-:E_{11}$ in a quantitative manner with temperature¹².

These results demonstrate how the NIR fluorescence of OCCs can be used to develop a nanothermometer and pH meter that might have direct applications for high-resolution sensing in complex, ultrasmall environments, such as those found in vivo. In this system, the SWCNT acts as a kind of fluorescent antenna to amplify small chemical changes that occur at the defect sites. We anticipate that many more OCC-based sensors could be developed using this model, particularly by taking advantage of the extensive number of bioconjugate reactions and the highly specific interactions of DNA and proteins.

Light sources.

The efficient radiative nature of OCCs suggests their potential as light sources for various applications, such as lasing and light-emitting diodes. For stimulated emission to occur, a lasing medium must support a population inversion, in which the number of filled excited states exceeds that at ground level. However, the electronic structure of unfunctionalized SWCNTs does not readily allow a population inversion to occur owing to the presence of dark exciton states below the bright singlet level, which promote rapid non-radiative relaxation back to the ground state^{71,115}, as well as efficient exciton–exciton annihilation, even at low excitation power densities⁹³. For this reason, non-radiative processes tend to dominate in SWCNTs (hence the low quantum yield), making the possibility of practical stimulated emission unlikely.

However, OCCs efficiently channel E_{11} dark excitons to the defect sites⁷. On the basis of DFT calculations of aryl OCCs, the defect state is intrinsically bright^{13,14}. In this scenario, we could envision pumping the system to the bright E_{11} excited state, which should be followed by rapid, non-radiative relaxation to the dark E_{11} exciton level, followed by capture (or direct transition from E_{11}) to the bright E_{11}^- state, which will radiatively recombine, thus supporting the conditions necessary for a population inversion to take place.

Supporting this theoretical hypothesis, Matsuda and colleagues⁹³ found evidence of population inversion in the presence of OCCs. The relative intensities of the E_{11} and E_{11}^- photoluminescence peaks show nonlinear behaviour as a function of the excitation power density. Monte Carlo simulations explained this trend by the rapid trapping of E_{11} excitons at the defect sites and the slow decay of the resulting E_{11}^- excitons that ultimately deplete the ground state, thus resulting in a population inversion. Calculations indicate that this condition could be achieved using a continuous-wave pump power density of just 40 kW cm^{-2} . By contrast, in unfunctionalized SWCNTs, a much higher excitation power density is required ($\sim 3 \times 10^4 \text{ kW cm}^{-2}$) to reach the same optical gain threshold⁹³. These findings suggest that OCC-functionalized SWCNTs could serve as a practical laser medium, although a more direct demonstration is still pending. On the basis of these results, we can envision an OCC-based SWCNT laser setup that could provide a source of coherent and monochromatic NIR light. Additionally, as we learn more ways of tuning the OCC state using optimized combinations of the semiconducting crystal host and the defect itself, it may be possible to push emission further into the mid-IR range.

Single-photon emitters.

OCCs are two-level systems that can be implanted in a semiconductor host, such as SWCNTs. The defect produces a deep trap that strongly localizes excitons, promoting single-photon emission at room temperature^{9,18}. Traditionally, single-photon emission has been achieved at either cryogenic temperatures¹¹⁶ or with nitrogen vacancies^{49–51} and 0D-confined materials such as quantum dots¹¹⁷. However, we note that these systems have never simultaneously achieved all the characteristics of an ideal quantum emitter for practical applications, including room-temperature, tunable, high-purity and high-yield single-photon emission at telecom wavelengths (TABLE 1). By contrast, OCCs in SWCNTs display all of these advantages^{7,9,18,108}, which make them particularly attractive as emerging quantum-light sources for applications in quantum information processing⁵¹, cryptography¹¹⁸ and communications¹¹⁹.

To achieve quantum communications, it is desirable to develop stable quantum emitters within the telecom wavelengths (1,260–1,625 nm). Doorn, Htoon and colleagues⁹ reported 99% purity single-photon emission from aryl-functionalized SWCNTs at room temperature. The combination of this versatile chemical approach plus the many available SWCNT chiralities enabled the generation of room-temperature single-photon emission that could be tuned across the entire telecom band, achieving $g^{(2)}(0)$ (a measure of photon antibunching, or the probability of more than one photon being emitted at a time) values as low as 0.01 (approaching the ideal limit of 0) at high laser pumping powers (1.5–2 μW) that approached the saturation of the OCC-induced photoluminescence intensity and with high single-photon count rates of $>10^5 \text{ s}^{-1}$ (REF.⁹) (FIG. 6c–e). For comparison, although pristine SWCNTs (without implanted defects) have also demonstrated single-photon emission capabilities at room temperature, the single photons are much less pure ($g^{(2)}(0) = 0.27$) and produced only at low excitation power (10 nW), which limits count rates¹²⁰. With established chemical approaches, we may be able to further optimize the quantum properties of OCCs and push the OCC photoluminescence peak further into the IR range using larger-diameter semiconducting SWCNTs and electron-withdrawing functional groups^{7,8}, or with the added help of defect-induced trion emission¹¹.

However, it should be noted that OCC-induced photoluminescence has been observed to blink under certain conditions, which will need to be better understood and suppressed to enhance the emission stability. The use of less-electron-withdrawing groups can reduce the blinking frequency and increase the stability of emission, possibly because functional groups that are more electron-withdrawing result in a larger dipole that can attract charged species in solutions that are well known to quench nanotube fluorescence (that is, the observed off-times between blinks). This hypothesis is consistent with the fact that OCC blinking increases as the pH of the solution is increased owing to the presence of charged hydroxide ions³⁶. Alternatively, solid-state^{35,121} or organic media (such as solvents and polymer matrices) may be used to prevent charged species from interfering with the E_{11}^- photoluminescence³⁶.

Towards future OCC technologies, techniques for aligning and patterning SWCNTs in semiconductor devices have been extensively studied^{122,123} and this knowledge may be applied for constructing semiconductor hosts for single-photon-emitting OCC arrays. The

next great hurdle will be developing methods of scalably patterning such defects on SWCNTs or other semiconductor host materials in a manner that is quantum-state-specific. The patterning of OCCs remains a significant challenge but may be achieved using light in resonance with the semiconductor substrate^{17,57,58} and established nanolithographic techniques^{124,125}.

Outlook

The future of OCCs is bright and we anticipate significant advances in the coming years on defect chemistry and physics, as well as applications. The ability to engineer the electronic properties of a crystal substrate through synthetic defects is a ground-breaking step for future directions of materials science and chemistry, but will depend on developing new defect-implanting reactions or adapting existing ones for the modification of SWCNTs and other materials. Serving as a molecular focal point, OCCs provide new, chemically tunable systems that open up opportunities to study the coupling of electrons, excitons, phonons and spin in low-dimensional materials and their effect on the electrical, optical, chemical and thermal properties of these materials, as well as enabling many potential applications (FIG. 7a).

Future OCC chemistries.

Already in these early stages of development, the number of OCCs that has currently been identified is high (~50 different functional groups) thanks to the molecular tunability achievable with diazonium salts, alkyl halides and the Billups–Birch reaction^{7,8,99}. We anticipate that other organic chemical reactions could be used to synthesize OCCs, including many that have already been well established on graphitic materials but not specifically explored for the creation of OCCs^{126–128}.

In this Review, we have primarily limited our discussion to reactions that form C–C bonds between the functional group and the graphitic materials. However, there is an extensive number of reactions that form C–F, C–Cl, C–N, C–O and C–S bonds to the nanotube surface^{126,127,129}. It is particularly interesting to note that before the discovery of OCCs oxygen doping was already known to produce a redshifted photoluminescence feature with respect to the pristine material^{37,38,97}. Although this defect type turns out to be intrinsically dark, its interpretation³⁸ and subsequent study by other research groups^{90,130} have provided a source of inspiration to the further development of OCCs.

An extensive search of host–OCC combinations may prove beneficial and, if nothing else, serve to provide a more complete understanding of defects. Divalent cycloaddition reactions may also be interesting to explore in depth as they result in some of the largest energy shifts of E_{11}^- relative to the E_{11} emission, thus pushing the fluorescence even further into the shortwave IR⁸, while also maintaining the π -conjugation of the nanotube, which may be important for retaining the electrical transport properties¹³¹ and the absorptive features necessary for optical excitation^{98,99}. Tailoring the functional groups with electron-withdrawing substituents is another way to further redshift the defect-induced photoluminescence towards telecom wavelengths⁹ and the NIR tissue-transparent window¹¹⁴. Additionally, it seems likely that the photophysics of OCCs will ultimately

depend on a rational combination of the defect and the semiconductor host²⁸. As we understand the structure–property relationship more deeply, the molecular tunability of OCCs may allow for designing and creating these synthetic defects in a specific quantum state. Conversely, these OCCs are tools themselves that allow for studying phenomena at the molecular level. OCCs have been used as chemical sensors for detecting species such as H⁺ and Ag⁺ (REFS^{12,26}). Bonding a molecule to the *sp*² lattice also induces characteristic photoluminescence that can be used as sensitive optical fingerprints to track chemical reactions^{7,8}. Because OCCs are quantum emitters, it may also be possible to achieve unprecedented sensitivity if entangled states can be designed and created for probing bond breaking and formation, as well as the detection of specific chemical perturbations.

Engineering the semiconducting host.

The optical properties of OCCs can be further tuned by judicious choice of the semiconducting crystal host. Using the electronic structural heterogeneity of SWCNTs to our advantage, we can more precisely tune the OCC photoluminescence. For example, we can select an SWCNT chirality featuring a convenient E_{11} bandgap that can be modified through the implantation of defects to achieve the desired emission wavelength. This prospect is becoming increasingly practical with recent advances in separation methods for the purification of single-chirality nanotube solutions^{78,132}.

We have largely limited our discussion to OCCs in SWCNTs because these systems have been well characterized, although there is no reason to believe that SWCNTs are unique in hosting this type of defect. We hypothesize that the OCC paradigm could be extended to virtually any semiconductor. Other materials that may host fluorescent OCCs include quasi-0D compounds such as graphene quantum dots^{133–136} and diamonds¹³⁷, other 1D systems such as silicon nanowires¹³⁸, as well as 2D materials¹³⁹ such as TMDs (for example, WSe₂, MoS₂, WS₂ and MoSe₂)^{43,45,46,140}, as shown in FIG. 7b, boron nitride allotropes^{141–143} and black phosphorus^{103,144}.

We note that defect-induced fluorescence has been observed in many of the systems listed above, but is typically attributed to exciton trapping by native defects, oxygen dopants and atomic vacancies^{44,45,145}, which, while fundamentally interesting, lack the molecular tunability of OCCs and, therefore, limit their potential for excitonic engineering. However, covalent functionalization of TMDs using organohalide reagents can convert the electronic material properties from metallic into semiconducting and simultaneously produce a new peak in the emission spectrum redshifted by ~200 meV from the native photoluminescence²⁰. Additionally, the intensity of this new emission can be tuned by increasing the defect density, all of which suggests the presence of OCC-like defects. This work shows that it should be possible to synthesize fluorescent defects in 2D materials, and yet, strangely, there have been few, if any, subsequent studies on the topic.

As the field is almost completely untapped, there is great opportunity to explore OCCs in semiconductor crystals beyond SWCNTs. A range of aryl functional groups can be employed to functionalize the basal plane (and not just native defects or edges) of MoS₂ by means of diazonium-based chemistry^{27,56,146}, although the optical properties of these chemical defects are unknown. The use of aryl functional groups to exfoliate black

phosphorus has also been explored using diazonium salts (forming C–P bonds to the surface), enabling the material's hole-carrier mobility to be tuned¹⁰³. However, while the excited state of monolayer black phosphorus (also called phosphorene) features highly anisotropic excitons (in this respect, behaving more like a 1D material akin to SWCNTs)¹⁴⁴, defect photoluminescence has not yet been observed — possibly because it has not been actively searched for.

In material systems in which the photoluminescence properties are somewhat well characterized, it is understandable that researchers tend to limit the range of emission wavelengths measured during spectroscopy, but this risks missing unexpected fluorescent features that may appear beyond the expected spectral window when covalent functional groups are added to the substrate. Additionally, similar to the case of SWCNTs, the defect density can greatly impact the intensity of OCC photoluminescence and, if it is not appropriately tuned, may cause researchers to miss these fluorescent features entirely, as was the case for SWCNTs for almost two decades⁷. Given what we now know about defects and the ability of OCCs to dramatically engineer a material's intrinsic electronic properties, it is perhaps timely to explore or re-examine many of these material systems and the roles of defects.

Future applications of OCCs.

As OCCs are largely unexplored, it is unsurprising that their potential applications have just started to emerge. In addition to sensing, light sources and single-photon emitters, as well as their immediate use as sensitive probes for understanding the physicochemical properties of defects themselves, we also envision these NIR emitters to be well suited for biological imaging applications.

Biological tissue scatters visible light and the absorption by water at ~950 nm further complicates the spectrum, but the NIR-II window (1,000–1,400 nm) is particularly effective for in vivo imaging, sensing or even light therapies owing to reduced scattering, water absorption and autofluorescence¹⁴⁷. SWCNTs have been considered promising candidates for bioimaging because of their remarkably narrow emission line (full width at half maximum ~23 meV at room temperature) and ability to fluoresce in a range of the NIR (~800–1,600 nm)¹⁴⁸ that effectively covers the NIR-II window¹⁴⁷. Additionally, unlike molecular fluorophores, SWCNTs are exceptionally photostable: they do not blink or photobleach under prolonged excitation¹⁴⁹. Researchers have already demonstrated that SWCNTs can be used as fluorophores for deep-tissue fluorescent imaging of tumours in mice¹¹⁴ and for tracking the extracellular space in living brains¹⁵⁰. However, the photon conversion efficiency is low in unfunctionalized SWCNTs⁷⁴ and the imaging resolution will also be ultimately limited by the length of the nanotubes, as the entire nanotube acts as a single fluorophore for imaging purposes.

Fluorescent OCCs present a natural solution to this problem, as they increase quantum yields by harvesting dark excitons⁷ and generate new emission features, including defect-trapped excitons and trions¹¹, both of which fluoresce in the NIR-II region (1,000–1,400 nm)¹⁴⁷, at which light can penetrate biological tissue with minimal scattering and low background autofluorescence. The generation of two or more photoluminescence features in

this window enables total NIR excitation and emission, which should improve bioimaging quality³⁸, as well as provide multimodal capabilities. Specifically, the E_{11} transition can be used to excite defect-induced E_{11}^- and trion fluorescence for total NIR excitation and emission¹¹. This attribute is beneficial for bioimaging as it circumvents the need to excite the material with visible wavelengths that can be strongly absorbed by biological tissues. Although in vivo biological imaging with SWCNTs has been demonstrated¹¹⁴, to our knowledge, there has been no study on the use of OCCs and defect-induced trion fluorescence for this purpose, despite the apparent potential. Furthermore, OCCs have allowed for ultrashort nanotubes to fluoresce brightly in the shortwave IR¹⁶, making it possible to improve the imaging resolution even further. We anticipate that these advantages of OCCs will further improve the intensity and resolution of future bioimaging results and note that this is another open area of research.

Open questions.

There are many basic questions surrounding OCCs that remain to be explored. For instance, what design principles should we heed when engineering OCCs to change a material's properties for a specific application? Also, how can we extend the concept of OCCs to other semiconducting materials? Resolving these questions will require extensive investigation of the structure–property relationships of OCCs, work that is currently underway in our laboratory as well as many others.

There is also still significant room to explore OCCs in SWCNTs. For example, how much do electron correlation and dark excitons contribute to the low quantum yield of nanotube photoluminescence? Is it possible to harness low-lying, triplet dark excitons using chemically engineered OCCs? What is the fundamental limit? How is the defect state coupled to that of the SWCNT? Is it phonon–dark exciton coupling as hypothesized^{7,13}? Or are there other mechanisms involved in governing defect-induced fluorescence? These problems are fundamentally important to understanding the excited state of this system and improving the light conversion efficiency critical to their applications for sensing, imaging, lighting and quantum information processing. Although we have made tremendous progress in this direction, further insights can be anticipated by applying advanced characterization tools, such as high-field magnetofluorescence spectroscopy and high-resolution resonance spectroscopy, as well as developing new ones for quantitative measurement at the single-defect level.

Additionally, how does the atomic arrangement of defects along a SWCNT affect fluorescence? Whether the functional groups are clustered or individually isolated, what arrangement generates the brightest features? Scanning tunnelling microscopy (STM) may be particularly well suited for resolving the atomic configuration of defects. With single-atom-tipped STM probes, it may be possible to image OCCs with atomic-scale resolution and correlate that information with the material's photoluminescence profile^{151–153}. Furthermore, STM luminescence, in which the injection of electrons at a defect site is used to stimulate the emission of photons, could enable in situ characterization of both defect configuration and emission^{154,155}.

At present, we also know very little about how OCCs respond to their environment outside of pH and temperature changes^{12,24,26}. How does a defect-trapped exciton respond to local chemical events? How sensitive and how selective can that be? Knowing that the OCC emission wavelength is strongly correlated with the Hammett constant of the molecular defect^{7,95}, we could anticipate the use of the defect-induced photoluminescence as a sensitive optical fingerprint for tracking various reactions that may be applied to modify the OCC on the host material. Additionally, the E_{11}^- peak can be used to measure the effect of other species (ions and molecules) in solution on the nanotube and its defects^{12,24}. Indeed, the possibilities of OCC-based chemistry are nearly limitless given the diversity of organic reactions available^{127,156}, but, at present, this remains a largely unexplored area of study.

Finally, there are fundamental questions that delve more deeply into the quantum physics of these nanomaterials. How can we use OCCs to generate indistinguishable single photons for quantum entanglement? Is it also possible to design spin-based qubits from OCCs? Uncovering the physics of the defect state, for instance, whether there is spin associated with defect-trapped trions or species that can be intentionally introduced to host an electron or nuclear spin at the OCC, will have particularly important implications for applications in quantum information. For instance, as trions feature non-zero spin, it may be possible to enable electrically driven OCC devices for spin manipulation by combining electrical generation¹⁵⁷ with defect-stabilized trions¹¹ under a magnetic field.

Theoretical modelling.

The studies of OCCs have substantially benefited from theoretical predictions. In particular, the groups led by Schatz and Tretiak have performed extensive theoretical calculations on many OCC systems, which have provided insightful guidance and helped to interpret experimental observations. Notably, time-dependent DFT calculations of OCC-functionalized SWCNTs reveal that the symmetry breaking of the carbon lattice by sp^3 defects asymmetrically splits the frontier orbitals of the SWCNT, creating new dipole-allowed optical transitions^{7,8,99}. Tretiak and colleagues have also shown that aryl-fluorescent OCCs localize the exciton's wavefunction in the vicinity of the defect, enhancing exciton-phonon coupling locally at a defect-induced potential well^{13,40}. The theoretical modelling also suggests the optical selection rules of emission for OCCs. Although the oxygen-induced excitonic state remains dark, the lowest excited state in OCCs is intrinsically bright and carries a large oscillator strength, making excitons efficiently fluoresce at these sp^3 quantum defects^{13,39}. DFT calculations also predict the effects of defect configuration and functionalization pattern (FIG. 7c). In particular, based on the charge distribution around OCCs, Mulliken analysis informs the likelihood of propagative functionalization to form bands of functional groups along the SWCNT or clusters near existing defects^{8,98}. The calculated stability and bandgap energy further predict the change in the electronic structure by the proximal defect configuration^{15,23,31}. Although, generally, time-dependent DFT does not properly capture the electronic correlation effects, appropriate density functionals and correction schemes are being developed and evaluated to provide insightful predictions on the excitonic effects in large conjugated systems^{41,158–161}.

Conclusion

In summary, OCCs have emerged as an entirely new class of quantum systems that can be chemically created in carbon nanotube semiconductors. A series of experiments and theoretical studies have revealed intriguing new physical properties that make these synthetic defects an exciting framework to explore new chemistry, physics, materials science, biomedical science and quantum technologies, as well as for previously unimagined applications. In this instance, the carbon nanotube is just a reactant and but one model system for the synthesis and study of OCCs. We envision that this unique defect type could be added to other materials for the creation of new systems with novel properties and a deeper understanding of defects and the underlying quantum effects.

Acknowledgements

This work was supported partially by the National Science Foundation (NSF) through grant PHY1839165. The authors are also grateful to the NSF (CHE1507974, which is continued as CHE1904488), the Air Force Office of Scientific Research (AFOSR; FA9550-16-1-0150) and the US National Institutes of Health (NIH)/National Institute of General Medical Sciences (NIGMS) (R01GM114167) for providing financial support to students and postdoctoral researchers who have participated in various aspects of the works cited in this Review.

References

1. Saito R, Dresselhaus G & Dresselhaus MS Physical Properties of Carbon Nanotubes (Imperial College Press, 1998).
2. De Volder MFL, Tawfick SH, Baughman RH & Hart AJ Carbon nanotubes: present and future commercial applications. *Science* 339, 535–539 (2013). [PubMed: 23372006]
3. Castro Neto AH, Guinea F, Peres NMR, Novoselov KS & Geim AK The electronic properties of graphene. *Rev. Mod. Phys* 81, 109–162 (2009).
4. Zhu Y et al. Graphene and graphene oxide: synthesis, properties, and applications. *Adv. Mater* 22, 3906–3924 (2010). [PubMed: 20706983]
5. Wang QH, Kalantar-Zadeh K, Kis A, Coleman JN & Strano MS Electronics and optoelectronics of two-dimensional transition metal dichalcogenides. *Nat. Nanotechnol* 7, 699–712 (2012). [PubMed: 23132225]
6. Chhowalla M et al. The chemistry of two-dimensional layered transition metal dichalcogenide nanosheets. *Nat. Chem* 5, 263–275 (2013). [PubMed: 23511414]
7. Piao Y et al. Brightening of carbon nanotube photoluminescence through the incorporation of sp³ defects. *Nat. Chem* 5, 840–845 (2013). [PubMed: 24056340]
8. Kwon H et al. Molecularly tunable fluorescent quantum defects. *J. Am. Chem. Soc* 138, 6878–6885 (2016). [PubMed: 27159413]
9. He X et al. Tunable room-temperature single-photon emission at telecom wavelengths from sp³ defects in carbon nanotubes. *Nat. Photon* 11, 577–582 (2017).
10. Wang QH & Strano MS Carbon nanotubes: a bright future for defects. *Nat. Chem* 5, 812–813 (2013). [PubMed: 24056334]
11. Brozena AH, Leeds JD, Zhang Y, Fourkas JT & Wang Y Controlled defects in semiconducting carbon nanotubes promote efficient generation and luminescence of trions. *ACS Nano* 8, 4239–4247 (2014). [PubMed: 24669843]
12. Kwon H et al. Optical probing of local pH and temperature in complex fluids with covalently functionalized, semiconducting carbon nanotubes. *J. Phys. Chem C* 119, 3733–3739 (2015).
13. Kim M et al. Fluorescent carbon nanotube defects manifest substantial vibrational reorganization. *J. Phys. Chem C* 120, 11268–11276 (2016).
14. Hartmann NF et al. Photoluminescence dynamics of aryl sp³ defect states in single-walled carbon nanotubes. *ACS Nano* 10, 8355–8365 (2016). [PubMed: 27529740]

15. He X et al. Low-temperature single carbon nanotube spectroscopy of sp³ quantum defects. *ACS Nano* 11, 10785–10796 (2017). [PubMed: 28958146]
16. Danné N et al. Ultrashort carbon nanotubes that fluoresce brightly in the near-infrared. *ACS Nano* 12, 6059–6065 (2018). [PubMed: 29889499]
17. Wu X, Kim M, Kwon H & Wang Y Photochemical creation of fluorescent quantum defects in semiconducting carbon nanotube hosts. *Angew. Chem. Int. Ed* 57, 648–653 (2018).
18. Srinivasan K & Zheng M Nanotube chemistry tunes light. *Nat. Photon* 11, 535–537 (2017).
19. Schrödinger E Versuch zur modellmässigen deutung des terms der scharfen nebenserien. *Z. Phys* 4, 347–354 (1921).
20. Voiry D et al. Covalent functionalization of monolayered transition metal dichalcogenides by phase engineering. *Nat. Chem* 7, 45–49 (2014). [PubMed: 25515889]
21. Maeda Y, Takehana Y, Yamada M, Suzuki M & Murakami T Control of the photoluminescence properties of single-walled carbon nanotubes by alkylation and subsequent thermal treatment. *Chem. Commun* 51, 13462–13465 (2015).
22. Jiang S et al. Tailoring the electronic structure of covalently functionalized germanane via the interplay of ligand strain and electronegativity. *Chem. Mater* 28, 8071–8077 (2016).
23. Shiraki T et al. Emergence of new red-shifted carbon nanotube photoluminescence based on proximal doped-site design. *Sci. Rep* 6, 28393 (2016). [PubMed: 27345862]
24. Shiraki T, Onitsuka H, Shiraishi T & Nakashima N Near infrared photoluminescence modulation of single-walled carbon nanotubes based on a molecular recognition approach. *Chem. Commun* 52, 12972–12975 (2016).
25. Shiraishi T, Shiraki T & Nakashima N Substituent effects on the redox states of locally functionalized single-walled carbon nanotubes revealed by in situ photoluminescence spectroelectrochemistry. *Nanoscale* 9, 16900–16907 (2017). [PubMed: 29077106]
26. Onitsuka H, Fujigaya T, Nakashima N & Shiraki T Control of the near infrared photoluminescence of locally functionalized single-walled carbon nanotubes via doping by azacrown-ether modification. *Chem. Eur. J* 24, 9393–9398 (2018). [PubMed: 29741218]
27. Chu XS et al. Direct covalent chemical functionalization of unmodified two-dimensional molybdenum disulfide. *Chem. Mater* 30, 2112–2128 (2018).
28. Kim M et al. Mapping structure–property relationships of organic color centers. *Chem* 4, 1–12 (2018).
29. Aota S, Akizuki N, Mouri S, Matsuda K & Miyauchi Y Upconversion photoluminescence imaging and spectroscopy of individual single-walled carbon nanotubes. *Appl. Phys. Express* 9, 045103 (2016).
30. Akizuki N, Aota S, Mouri S, Matsuda K & Miyauchi Y Efficient near-infrared up-conversion photoluminescence in carbon nanotubes. *Nat. Commun* 6, 8920 (2015). [PubMed: 26568250]
31. Saha A et al. Narrow-band single-photon emission through selective aryl functionalization of zigzag carbon nanotubes. *Nat. Chem* 10, 1089–1095 (2018). [PubMed: 30177779]
32. Goldsmith BR et al. Conductance-controlled point functionalization of single-walled carbon nanotubes. *Science* 315, 77–81 (2007). [PubMed: 17204645]
33. Wilson H et al. Electrical monitoring of sp³ defect formation in individual carbon nanotubes. *J. Phys. Chem C* 120, 1971–1976 (2016).
34. Maciel IO et al. Electron and phonon renormalization near charged defects in carbon nanotubes. *Nat. Mater* 7, 878–883 (2008). [PubMed: 18931672]
35. Ma X, Hartmann NF, Baldwin JKS, Doorn SK & Htoon H Room-temperature single-photon generation from solitary dopants of carbon nanotubes. *Nat. Nanotechnol* 10, 671–675 (2015). [PubMed: 26167766]
36. Hartmann NF et al. Photoluminescence imaging of solitary dopant sites in covalently doped single-wall carbon nanotubes. *Nanoscale* 7, 20521–20530 (2015). [PubMed: 26586162]
37. Harutyunyan H et al. Defect-induced photoluminescence from dark excitonic states in individual single-walled carbon nanotubes. *Nano Lett.* 9, 2010–2014 (2009). [PubMed: 19331347]

38. Ghosh S, Bachilo SM, Simonette RA, Beckingham KM & Weisman RB Oxygen doping modifies near-infrared band gaps in fluorescent single-walled carbon nanotubes. *Science* 330, 1656–1659 (2010). [PubMed: 21109631]
39. Kilina S, Ramirez J & Tretiak S Brightening of the lowest exciton in carbon nanotubes via chemical functionalization. *Nano Lett.* 12, 2306–2312 (2012). [PubMed: 22494501]
40. Gifford BJ, Kilina S, Htoon H, Doorn SK & Tretiak S Exciton localization and optical emission in aryl-functionalized carbon nanotubes. *J. Phys. Chem C* 122, 1828–1838 (2018).
41. Gifford BJ et al. Correction scheme for comparison of computed and experimental optical transition energies in functionalized single-walled carbon nanotubes. *J. Phys. Chem. Lett* 9, 2460–2468 (2018). [PubMed: 29678108]
42. Glückert JT et al. Dipolar and charged localized excitons in carbon nanotubes. *Phys. Rev. B* 98, 195413 (2018).
43. Nan H et al. Strong photoluminescence enhancement of MoS₂ through defect engineering and oxygen bonding. *ACS Nano* 8, 5738–5745 (2014). [PubMed: 24836121]
44. Tongay S et al. Defects activated photoluminescence in two-dimensional semiconductors: interplay between bound, charged, and free excitons. *Sci. Rep* 3, 2657 (2013). [PubMed: 24029823]
45. Chow PK et al. Defect-induced photoluminescence in monolayer semiconducting transition metal dichalcogenides. *ACS Nano* 9, 1520–1527 (2015). [PubMed: 25603228]
46. Yore AE et al. Visualization of defect-induced excitonic properties of the edges and grain boundaries in synthesized monolayer molybdenum disulfide. *J. Phys. Chem C* 120, 24080–24087 (2016).
47. Galland C & Imamoglu A All-optical manipulation of electron spins in carbon-nanotube quantum dots. *Phys. Rev. Lett* 101, 157404 (2008). [PubMed: 18999640]
48. Fan Y, Goldsmith BR & Collins PG Identifying and counting point defects in carbon nanotubes. *Nat. Mater* 4, 906–911 (2005). [PubMed: 16267574]
49. Beveratos A et al. Single photon quantum cryptography. *Phys. Rev. Lett* 89, 187901 (2002). [PubMed: 12398636]
50. Inam FA et al. Emission and nonradiative decay of nanodiamond NV centers in a low refractive index environment. *ACS Nano* 7, 3833–3843 (2013). [PubMed: 23586780]
51. Kurtsiefer C, Mayer S, Zarda P & Weinfurter H Stable solid-state source of single photons. *Phys. Rev. Lett* 85, 290–293 (2000). [PubMed: 10991265]
52. Resch-Genger U, Grabolle M, Cavaliere-Jaricot S, Nitschke R & Nann T Quantum dots versus organic dyes as fluorescent labels. *Nat. Methods* 5, 763–775 (2008). [PubMed: 18756197]
53. Zhang M et al. Bright quantum dots emitting at ~1,600 nm in the NIR-IIb window for deep tissue fluorescence imaging. *Proc. Natl Acad. Sci. USA* 115, 6590–6595 (2018). [PubMed: 29891702]
54. Senellart P, Solomon G & White A High-performance semiconductor quantum-dot single-photon sources. *Nat. Nanotechnol* 12, 1026–1039 (2017). [PubMed: 29109549]
55. Castelletto S et al. A silicon carbide room-temperature single-photon source. *Nat. Mater* 13, 151–156 (2013). [PubMed: 24240243]
56. Knirsch KC et al. Basal-plane functionalization of chemically exfoliated molybdenum disulfide by diazonium salts. *ACS Nano* 9, 6018–6030 (2015). [PubMed: 25969861]
57. Powell LR, Piao Y & Wang Y Optical excitation of carbon nanotubes drives localized diazonium reactions. *J. Phys. Chem. Lett* 7, 3690–3694 (2016). [PubMed: 27588432]
58. Powell LR, Kim M & Wang Y Chirality-selective functionalization of semiconducting carbon nanotubes with a reactivity-switchable molecule. *J. Am. Chem. Soc* 139, 12533–12540 (2017). [PubMed: 28844140]
59. Shiraki T, Uchimura S, Shiraishi T, Onitsuka H & Nakashima N Near infrared photoluminescence modulation by defect site design using aryl isomers in locally functionalized single-walled carbon nanotubes. *Chem. Commun* 53, 12544–12547 (2017).
60. Maultzsch J et al. Exciton binding energies in carbon nanotubes from two-photon photoluminescence. *Phys. Rev. B* 72, 241402 (2005).
61. Berber S, Kwon Y-K & Tománek D Unusually high thermal conductivity of carbon nanotubes. *Phys. Rev. Lett* 84, 4613–4616 (2000). [PubMed: 10990753]

62. Dürkop T, Getty SA, Cobas E & Fuhrer MS Extraordinary mobility in semiconducting carbon nanotubes. *Nano Lett.* 4, 35–39 (2004).
63. Du X, Skachko I, Barker A & Andrei EY Approaching ballistic transport in suspended graphene. *Nat. Nanotechnol* 3, 491–495 (2008).
64. Fujii M et al. Measuring the thermal conductivity of a single carbon nanotube. *Phys. Rev. Lett* 95, 065502 (2005). [PubMed: 16090962]
65. Balandin AA et al. Superior thermal conductivity of single-layer graphene. *Nano Lett.* 8, 902–907 (2008). [PubMed: 18284217]
66. Crochet JJ, Duque JG, Werner JH & Doorn SK Photoluminescence imaging of electronic-impurity-induced exciton quenching in single-walled carbon nanotubes. *Nat. Nanotechnol* 7, 126–132 (2012).
67. Manzoni C et al. Intersubband exciton relaxation dynamics in single-walled carbon nanotubes. *Phys. Rev. Lett* 94, 207401 (2005). [PubMed: 16090288]
68. Wang F, Dukovic G, Brus LE & Heinz TF The optical resonances in carbon nanotubes arise from excitons. *Science* 308, 838–841 (2005). [PubMed: 15879212]
69. Zhao H & Mazumdar S Electron–electron interaction effects on the optical excitations of semiconducting single-walled carbon nanotubes. *Phys. Rev. Lett* 93, 157402 (2004). [PubMed: 15524940]
70. Ando T Effects of valley mixing and exchange on excitons in carbon nanotubes with Aharonov–Bohm flux. *J. Phys. Soc. Jpn* 75, 024707 (2006).
71. Spataru CD, Ismail-Beigi S, Capaz RB & Louie SG Theory and ab initio calculation of radiative lifetime of excitons in semiconducting carbon nanotubes. *Phys. Rev. Lett* 95, 247402 (2005). [PubMed: 16384422]
72. Berciaud S, Cognet L & Lounis B Luminescence decay and the absorption cross section of individual single-walled carbon nanotubes. *Phys. Rev. Lett* 101, 077402 (2008). [PubMed: 18764579]
73. Srivastava A, Htoon H, Klimov VI & Kono J Direct observation of dark excitons in individual carbon nanotubes: inhomogeneity in the exchange splitting. *Phys. Rev. Lett* 101, 087402 (2008). [PubMed: 18764659]
74. Lee AJ et al. Bright fluorescence from individual single-walled carbon nanotubes. *Nano Lett.* 11, 1636–1640 (2011). [PubMed: 21417364]
75. Cognet L et al. Stepwise quenching of exciton fluorescence in carbon nanotubes by single-molecule reactions. *Science* 316, 1465–1468 (2007). [PubMed: 17556581]
76. Kelly A & Knowles KM *Crystallography and Crystal Defects* (John Wiley & Sons, 2012).
77. Charlier JC Defects in carbon nanotubes. *Acc. Chem. Res* 35, 1063–1069 (2002). [PubMed: 12484794]
78. Hersam MC Progress towards monodisperse single-walled carbon nanotubes. *Nat. Nanotechnol* 3, 387–394 (2008).
79. Wang P et al. Superacid-surfactant exchange: enabling nondestructive dispersion of full-length carbon nanotubes in water. *ACS Nano* 11, 9231–9238 (2017). [PubMed: 28792746]
80. Dukovic G et al. Reversible surface oxidation and efficient luminescence quenching in semiconductor single-wall carbon nanotubes. *J. Am. Chem. Soc* 126, 15269–15276 (2004). [PubMed: 15548024]
81. Hertel T, Himmelein S, Ackermann T, Stich D & Crochet J Diffusion limited photoluminescence quantum yields in 1D semiconductors: single-wall carbon nanotubes. *ACS Nano* 4, 7161–7168 (2010). [PubMed: 21105744]
82. Harrah DM & Swan AK The role of length and defects on optical quantum efficiency and exciton decay dynamics in single-walled carbon nanotubes. *ACS Nano* 5, 647–655 (2011). [PubMed: 21166468]
83. Collins PG in *Oxford Handbook of Nanoscience & Technology* (eds Narlikar AV & Fu YY) 31–93 (Oxford Univ. Press, 2010).
84. Queisser HJ & Haller EE Defects in semiconductors: some fatal, some vital. *Science* 281, 945–950 (1998). [PubMed: 9703502]

85. Banhart F, Kotakoski J & Krasheninnikov AV Structural defects in graphene. *ACS Nano* 5, 26–41 (2011). [PubMed: 21090760]
86. Mandel L Sub-Poissonian photon statistics in resonance fluorescence. *Opt. Lett* 4, 205–207 (1979). [PubMed: 19687850]
87. Powell LR, Piao Y, Ng AL & Wang Y Channeling excitons to emissive defect sites in carbon nanotube semiconductors beyond the dilute regime. *J. Phys. Chem. Lett* 9, 2803–2807 (2018). [PubMed: 29746778]
88. Ramirez J, Mayo ML, Kilina S & Tretiak S Electronic structure and optical spectra of semiconducting carbon nanotubes functionalized by diazonium salts. *Chem. Phys* 413, 89–101 (2013).
89. Takagahara T & Hanamura E Giant-oscillatorstrength effect on excitonic optical nonlinearities due to localization. *Phys. Rev. Lett* 56, 2533–2536 (1986). [PubMed: 10033017]
90. Miyauchi Y et al. Brightening of excitons in carbon nanotubes on dimensionality modification. *Nat. Photon* 7, 715–719 (2013).
91. Citrin DS Long intrinsic radiative lifetimes of excitons in quantum wires. *Phys. Rev. Lett* 69, 3393–3396 (1992). [PubMed: 10046807]
92. Mouri S, Miyauchi Y, Iwamura M & Matsuda K Temperature dependence of photoluminescence spectra in hole-doped single-walled carbon nanotubes: Implications of trion localization. *Phys. Rev. B* 87, 045408 (2013).
93. Iwamura M et al. Nonlinear photoluminescence spectroscopy of carbon nanotubes with localized exciton states. *ACS Nano* 8, 11254–11260 (2014). [PubMed: 25331628]
94. Shaver J et al. Magnetic brightening of carbon nanotube photoluminescence through symmetry breaking. *Nano Lett.* 7, 1851–1855 (2007). [PubMed: 17542638]
95. Hansch C, Leo A & Taft RW A survey of Hammett substituent constants and resonance and field parameters. *Chem. Rev* 91, 165–195 (1991).
96. Iakoubovskii K et al. Midgap luminescence centers in single-wall carbon nanotubes created by ultraviolet illumination. *Appl. Phys. Lett* 89, 173108 (2006).
97. McDonald TJ, Blackburn JL, Metzger WK, Rumbles G & Heben MJ Chiral-selective protection of single-walled carbon nanotube photoluminescence by surfactant selection. *J. Phys. Chem C* 111, 17894–17900 (2007).
98. Deng S et al. Confined propagation of covalent chemical reactions on single-walled carbon nanotubes. *Nat. Commun* 2, 382 (2011). [PubMed: 21750536]
99. Zhang Y et al. Propagative sidewall alkylcarboxylation that induces red-shifted near-IR photoluminescence in single-walled carbon nanotubes. *J. Phys. Chem. Lett* 4, 826–830 (2013). [PubMed: 26281939]
100. Strano MS et al. Electronic structure control of single-walled carbon nanotube functionalization. *Science* 301, 1519–1522 (2003). [PubMed: 12970561]
101. An L, Fu Q, Lu C & Liu J A simple chemical route to selectively eliminate metallic carbon nanotubes in nanotube network devices. *J. Am. Chem. Soc* 126, 10520–10521 (2004). [PubMed: 15327292]
102. Kaplan A et al. Current and future directions in electron transfer chemistry of graphene. *Chem. Soc. Rev* 46, 4530–4571 (2017). [PubMed: 28621376]
103. Ryder CR et al. Covalent functionalization and passivation of exfoliated black phosphorus via aryl diazonium chemistry. *Nat. Chem* 8, 597–602 (2016). [PubMed: 27219705]
104. Schmidt G, Gallon S, Esnouf S, Bourgoin JP & Chenevier P Mechanism of the coupling of diazonium to single-walled carbon nanotubes and its consequences. *Chem. Eur. J* 15, 2101–2110 (2009). [PubMed: 19142944]
105. Usrey ML, Lippmann ES & Strano MS Evidence for a two-step mechanism in electronically selective single-walled carbon nanotube reactions. *J. Am. Chem. Soc* 127, 16129–16135 (2005). [PubMed: 16287300]
106. Qin S et al. Solubilization and purification of single-wall carbon nanotubes in water by in situ radical polymerization of sodium 4-styrenesulfonate. *Macromolecules* 37, 3965–3967 (2004).

107. Crochet JJ et al. Disorder limited exciton transport in colloidal single-wall carbon nanotubes. *Nano Lett.* 12, 5091–5096 (2012). [PubMed: 22985181]
108. He X et al. Carbon nanotubes as emerging quantum-light sources. *Nat. Mater* 17, 663–670 (2018). [PubMed: 29915427]
109. Robinson JA, Snow ES, Badescu SC, Reinecke TL & Perkins FK Role of defects in single-walled carbon nanotube chemical sensors. *Nano Lett.* 6, 1747–1751 (2006). [PubMed: 16895367]
110. Barone PW, Baik S, Heller DA & Strano MS Near-infrared optical sensors based on single-walled carbon nanotubes. *Nat. Mater* 4, 86–92 (2004). [PubMed: 15592477]
111. Heller DA et al. Optical detection of DNA conformational polymorphism on single-walled carbon nanotubes. *Science* 311, 508–511 (2006). [PubMed: 16439657]
112. Harvey JD, Baker HA, Mercer E, Budhathoki-Uprety J & Heller DA Control of carbon nanotube solvatochromic response to chemotherapeutic agents. *ACS Appl. Mater. Interfaces* 9, 37947–37953 (2017). [PubMed: 29048868]
113. Williams RM, Lee C & Heller DA A fluorescent carbon nanotube sensor detects the metastatic prostate cancer biomarker uPA. *ACS Sens.* 3, 1838–1845 (2018). [PubMed: 30169018]
114. Hong G, Diao S, Antaris AL & Dai H Carbon nanomaterials for biological imaging and nanomedicinal therapy. *Chem. Rev* 115, 10816–10906 (2015). [PubMed: 25997028]
115. Scholes GD et al. Low-lying exciton states determine the photophysics of semiconducting single wall carbon nanotubes. *J. Phys. Chem C* 111, 11139–11149 (2007).
116. Högele A, Galland C, Winger M & Imamoglu A Photon antibunching in the photoluminescence spectra of a single carbon nanotube. *Phys. Rev. Lett* 100, 217401 (2008). [PubMed: 18518631]
117. Kako S et al. A gallium nitride single-photon source operating at 200 K. *Nat. Mater* 5, 887–892 (2006). [PubMed: 17057699]
118. Gisin N, Ribordy G, Tittel W & Zbinden H Quantum cryptography. *Rev. Mod. Phys* 74, 145–195 (2002).
119. Gisin N & Thew R Quantum communication. *Nat. Photon* 1, 165–171 (2007).
120. Ishii A, Uda T & Kato YK Room-temperature single-photon emission from micrometer-long air-suspended carbon nanotubes. *Phys. Rev. Appl* 8, 054039 (2017).
121. Ma X, Baldwin JKS, Hartmann NF, Doorn SK & Htoon H Solid-state approach for fabrication of photostable, oxygen-doped carbon nanotubes. *Adv. Func. Mater* 25, 6157–6164 (2015).
122. Cao Q & Han S-J Single-walled carbon nanotubes for high-performance electronics. *Nanoscale* 5, 8852–8863 (2013). [PubMed: 23921893]
123. Cao Q, Tersoff J, Farmer DB, Zhu Y & Han S-J Carbon nanotube transistors scaled to a 40-nanometer footprint. *Science* 356, 1369–1372 (2017). [PubMed: 28663497]
124. Salaita K, Wang Y & Mirkin CA Applications of dip-pen nanolithography. *Nat. Nanotechnol* 2, 145–155 (2007). [PubMed: 18654244]
125. Huang Z et al. Photoactuated pens for molecular printing. *Adv. Mater* 30, 1705303 (2018).
126. Dyke CA & Tour JM Covalent functionalization of single-walled carbon nanotubes for materials applications. *J. Phys. Chem. A* 108, 11151–11159 (2004).
127. Tasis D, Tagmatarchis N, Bianco A & Prato M Chemistry of carbon nanotubes. *Chem. Rev* 106, 1105–1136 (2006). [PubMed: 16522018]
128. Quintana M, Vazquez E & Prato M Organic functionalization of graphene in dispersions. *Acc. Chem. Res* 46, 138–148 (2013). [PubMed: 22872046]
129. Peng F, Zhang L, Wang H, Lv P & Yu H Sulfonated carbon nanotubes as a strong protonic acid catalyst. *Carbon* 43, 2405–2408 (2005).
130. Ma X et al. Electronic structure and chemical nature of oxygen dopant states in carbon nanotubes. *ACS Nano* 8, 10782–10789 (2014). [PubMed: 25265272]
131. Park H, Zhao J & Lu JP Effects of sidewall functionalization on conducting properties of single wall carbon nanotubes. *Nano Lett.* 6, 916–919 (2006). [PubMed: 16683825]
132. Ao G & Zheng M Preparation and separation of DNA-wrapped carbon nanotubes. *Curr. Protoc. Chem. Biol* 7, 43–51 (2017).
133. Zhu S et al. Graphene quantum dots with controllable surface oxidation, tunable fluorescence and up-conversion emission. *RSC Adv.* 2, 2717–2720 (2012).

134. Wang L et al. Common origin of green luminescence in carbon nanodots and graphene quantum dots. *ACS Nano* 8, 2541–2547 (2014). [PubMed: 24517361]
135. Zhu S et al. Surface chemistry routes to modulate the photoluminescence of graphene quantum dots: from fluorescence mechanism to up-conversion bioimaging applications. *Adv. Func. Mater* 22, 4732–4740 (2012).
136. Feng L et al. Propagative exfoliation of high quality graphene. *Chem. Mater* 25, 4487–4496 (2013).
137. Tisler J et al. Fluorescence and spin properties of defects in single digit nanodiamonds. *ACS Nano* 3, 1959–1965 (2009). [PubMed: 21452865]
138. Sivakov VA, Voigt F, Berger A, Bauer G & Christiansen SH Roughness of silicon nanowire sidewalls and room temperature photoluminescence. *Phys. Rev. B* 82, 125446 (2010).
139. Mannix AJ, Kiraly B, Hersam MC & Guisinger NP Synthesis and chemistry of elemental 2D materials. *Nat. Rev. Chem* 1, 0014 (2017).
140. Chakraborty C, Kinnischtzke L, Goodfellow KM, Beams R & Vamivakas AN Voltage-controlled quantum light from an atomically thin semiconductor. *Nat. Nanotechnol* 10, 507–511 (2015). [PubMed: 25938569]
141. Museur L, Feldbach E & Kanaev A Defect-related photoluminescence of hexagonal boron nitride. *Phys. Rev. B* 78, 155204 (2008).
142. Tran TT, Bray K, Ford MJ, Toth M & Aharonovich I Quantum emission from hexagonal boron nitride monolayers. *Nat. Nanotechnol* 11, 37–41 (2015). [PubMed: 26501751]
143. Grosso G et al. Tunable and high-purity room temperature single-photon emission from atomic defects in hexagonal boron nitride. *Nat. Commun* 8, 705 (2017). [PubMed: 28951591]
144. Wang X et al. Highly anisotropic and robust excitons in monolayer black phosphorus. *Nat. Nanotechnol* 10, 517 (2015).
145. Martínez LJ et al. Efficient single photon emission from a high-purity hexagonal boron nitride crystal. *Phys. Rev. B* 94, 121405 (2016).
146. Benson EE et al. Balancing the hydrogen evolution reaction, surface energetics, and stability of metallic MoS₂ nanosheets via covalent functionalization. *J. Am. Chem. Soc* 140, 441–450 (2018). [PubMed: 29281274]
147. Welsher K et al. A route to brightly fluorescent carbon nanotubes for near-infrared imaging in mice. *Nat. Nanotechnol* 4, 773–780 (2009). [PubMed: 19893526]
148. Bachilo SM et al. Structure-assigned optical spectra of single-walled carbon nanotubes. *Science* 298, 2361–2366 (2002). [PubMed: 12459549]
149. Heller DA, Baik S, Eurell TE & Strano MS Single-walled carbon nanotube spectroscopy in live cells: towards long-term labels and optical sensors. *Adv. Mater* 17, 2793–2799 (2005).
150. Godin AG et al. Single-nanotube tracking reveals the nanoscale organization of the extracellular space in the live brain. *Nat. Nanotechnol* 12, 238–243 (2016).
151. Gross L Recent advances in submolecular resolution with scanning probe microscopy. *Nat. Chem* 3, 273–278 (2011). [PubMed: 21430684]
152. Mohn F, Schuler B, Gross L & Meyer G Different tips for high-resolution atomic force microscopy and scanning tunneling microscopy of single molecules. *Appl. Phys. Lett* 102, 073109 (2013).
153. Wong D et al. Characterization and manipulation of individual defects in insulating hexagonal boron nitride using scanning tunnelling microscopy. *Nat. Nanotechnol* 10, 949–953 (2015). [PubMed: 26301901]
154. Rossel F, Pivetta M & Schneider W-D Luminescence experiments on supported molecules with the scanning tunneling microscope. *Surf. Sci. Rep* 65, 129–144 (2010).
155. Zhang C et al. Fabrication of silver tips for scanning tunneling microscope induced luminescence. *Rev. Sci. Instrum* 82, 083101 (2011). [PubMed: 21895227]
156. Bahr JL & Tour JM Covalent chemistry of single-wall carbon nanotubes. *J. Mater. Chem* 12, 1952–1958 (2002).
157. Liang S et al. Solid state carbon nanotube device for controllable trion electroluminescence emission. *Nanoscale* 8, 6761–6769 (2016). [PubMed: 26953676]

158. Igumenshchev KI, Tretiak S & Chernyak VY Excitonic effects in a time-dependent density functional theory. *J. Chem. Phys* 127, 114902 (2007). [PubMed: 17887875]
159. Yang Z-h, Li, Y. & Ullrich, C. A. A minimal model for excitons within time-dependent density-functional theory. *J. Chem. Phys* 137, 014513 (2012). [PubMed: 22779671]
160. Mewes SA, Plasser F, Krylov A & Dreuw A Benchmarking excited-state calculations using exciton properties. *J. Chem. Theory Comput* 14, 710–725 (2018). [PubMed: 29323887]
161. Turkowski V, Din UN & Rahman ST Time-dependent density-functional theory and excitons in bulk and two-dimensional semiconductors. *Computation* 5, 39 (2017).

Single photon

Photons that exhibit photon antibunching, such that it can be considered as emitting one at a time.

Author Manuscript

Author Manuscript

Author Manuscript

Author Manuscript

Quantum defects

Chemical defects that exhibit well-defined quantum mechanical characteristics, such as single-photon emission, and that may be described as a two-level system.

Author Manuscript

Author Manuscript

Author Manuscript

Author Manuscript

Organic colour centres

(OCC). Photon-emitting centres induced by covalently bonding organic molecules onto a host crystal.

Author Manuscript

Author Manuscript

Author Manuscript

Author Manuscript

Dark exciton

An exciton forms when an electron and a hole are bound together by the Coulomb interaction. Dark excitons are not optically allowed as they recombine non-radiatively.

Author Manuscript

Author Manuscript

Author Manuscript

Author Manuscript

Van Hove singularities

Singularities in the density of states of a crystal, named after the belgian physicist Léon Van Hove.

Author Manuscript

Author Manuscript

Author Manuscript

Author Manuscript

Chirality

A general structural identifier of single-walled carbon nanotubes, referencing the nanotube's chiral roll-up vector and indicative of the material's diameter and electronic structure. each chirality can be indexed by a pair of integers (n,m) and may include an additional label, if required, to differentiate its left-handed or right-handed helicity.

Taft constant

An empirical constant that describes the relative steric, inductive and resonance effects of substituents.

Photon antibunching

The lack of simultaneous emission of more than two photons at a time.

Author Manuscript

Author Manuscript

Author Manuscript

Author Manuscript

Hammett constant

An empirical constant that describes the relative inductive effect of a substituent of benzene derivatives.

Author Manuscript

Author Manuscript

Author Manuscript

Author Manuscript

Mulliken population analysis

A computational method used to estimate the partial charges on atoms in a molecule or material system.

Author Manuscript

Author Manuscript

Author Manuscript

Author Manuscript

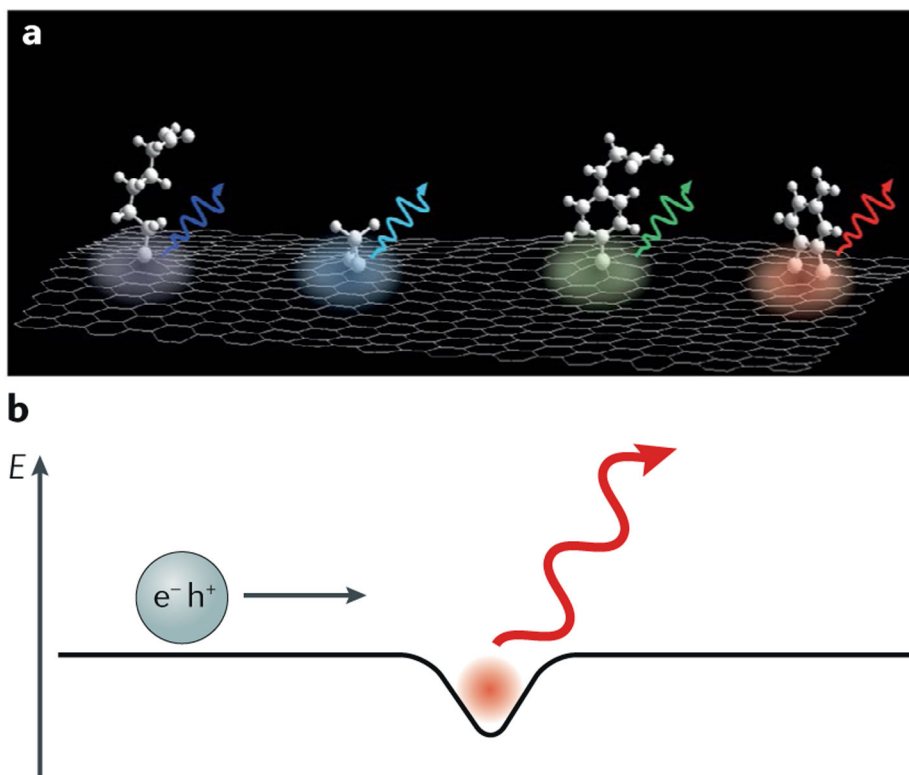


Fig. 1 | Organic colour centres in a semiconductor host.

a | Organic colour centres are quantum emitters that can be synthesized by covalently attaching organic functional groups to a semiconducting host, in this case, a single-walled carbon nanotube (SWCNT). **b** | The organic functional group acts as a defect on the SWCNT and produces a localized quantum well in which mobile excitons from the host semiconductor are trapped and efficiently recombine to emit single photons. Part **a** is adapted with permission from REF.⁸, ACS.

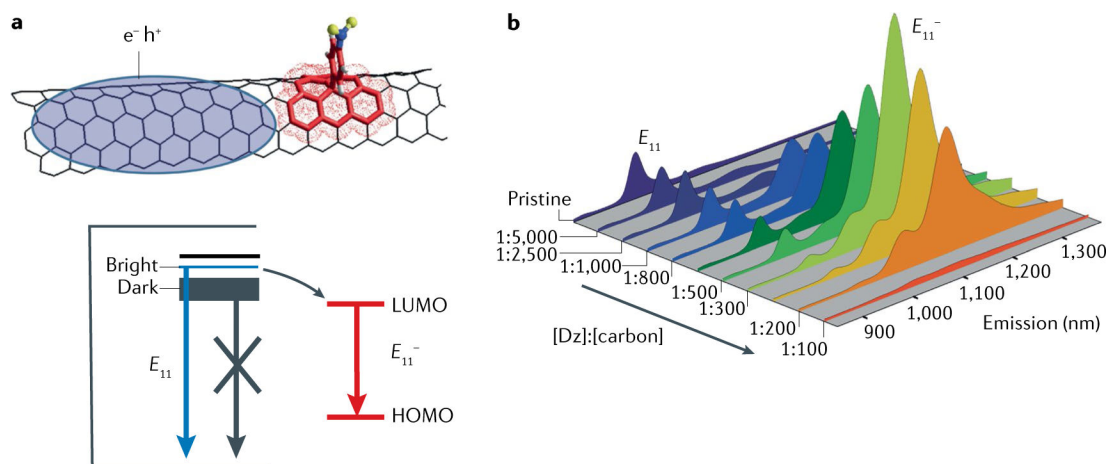


Fig. 2 |. Optical properties of organic colour centres.

An organic colour centre creates a localized two-level state in the single-walled carbon nanotube (SWCNT) host, introducing new chemical functionality and optical properties. **a** | Covalent bonding of an aryl functional group to the sidewall of a (6,5)-SWCNT creates a two-level state that enables dark excitons from the host to be harnessed. The band structure and theoretically predicted excitonic states for the functionalized SWCNT feature bright singlet and dark E_{11} excitons of the SWCNT host (in blue and black, respectively) and the E_{11}^- state (red) generated from the sp^3 molecular defect. **b** | Defect-induced photoluminescence (E_{11}^-) arises as more 4-nitrobenzene organic colour centres are incorporated into (6,5)-SWCNTs through a reaction using diazonium salts. Part **a** and data for part **b** are adapted from REF.⁷, Springer Nature Limited.

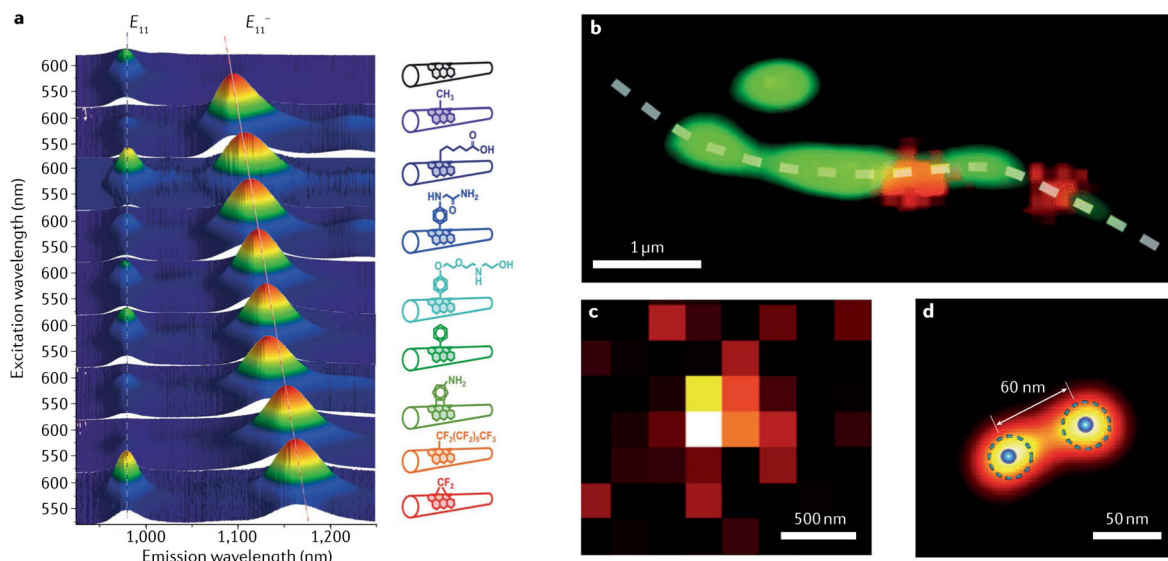


Fig. 3 |. Key evidence of exciton trapping by organic colour centres.

a | Organic colour centre (OCC) photoluminescence can be tuned through the incorporation of various functionalities to the surface of single-walled carbon nanotubes (SWCNTs). **b** | Photoluminescence arising from the E_{11} transition (green) and E_{11}^- transition (red) along an individual (6,5)-SWCNT- $C_6H_4OCH_3$ (position indicated by the dashed line). The OCC photoluminescence is spatially isolated and spectrally distinct from the native emission of the nanotube. **c** | Diffraction-limited E_{11}^- photoluminescence image of an ultrashort (6,5)-SWCNT- C_6F_{13} , in which the individual location of the defect(s) cannot be resolved. **d** | Super-localization of fluorescent OCCs on (6,5)-SWCNT- C_6F_{13} displays two super-resolved perfluorohexyl chain ($-C_6F_{13}$) defects at the SWCNT ends. Part **a** is adapted with permission from REF.⁸, ACS. Part **b** is adapted with permission from REF.³⁶, RSC. Parts **c** and **d** are adapted with permission from REF.¹⁶, ACS.

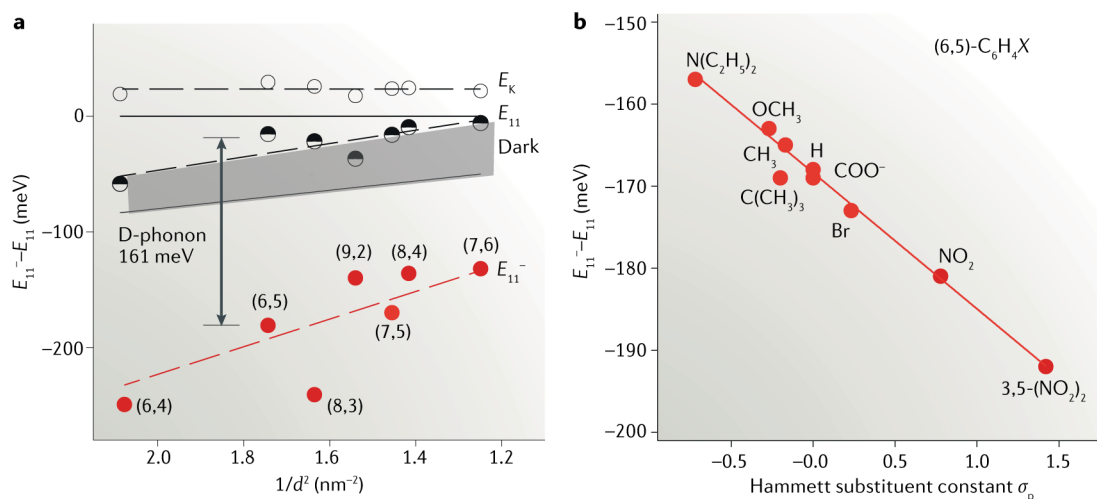


Fig. 4 | Dark exciton harvesting at fluorescent organic colour centres.

a | The energy shift between the E_{11} and E_{11}^- emissions as a function of the nanotube chirality diameter approximately corresponds to the energy of the D-phonon mode associated with defect sites in the nanotube structure. This suggests that exciton–phonon coupling enhances dark exciton brightening by the organic colour centre. **b** | The redshift of E_{11}^- is enhanced by the use of electron-withdrawing substituents of aryl-functionalized (6,5)-single-walled carbon nanotubes. Reproduced with permission from REF.⁷, Springer Nature Limited.

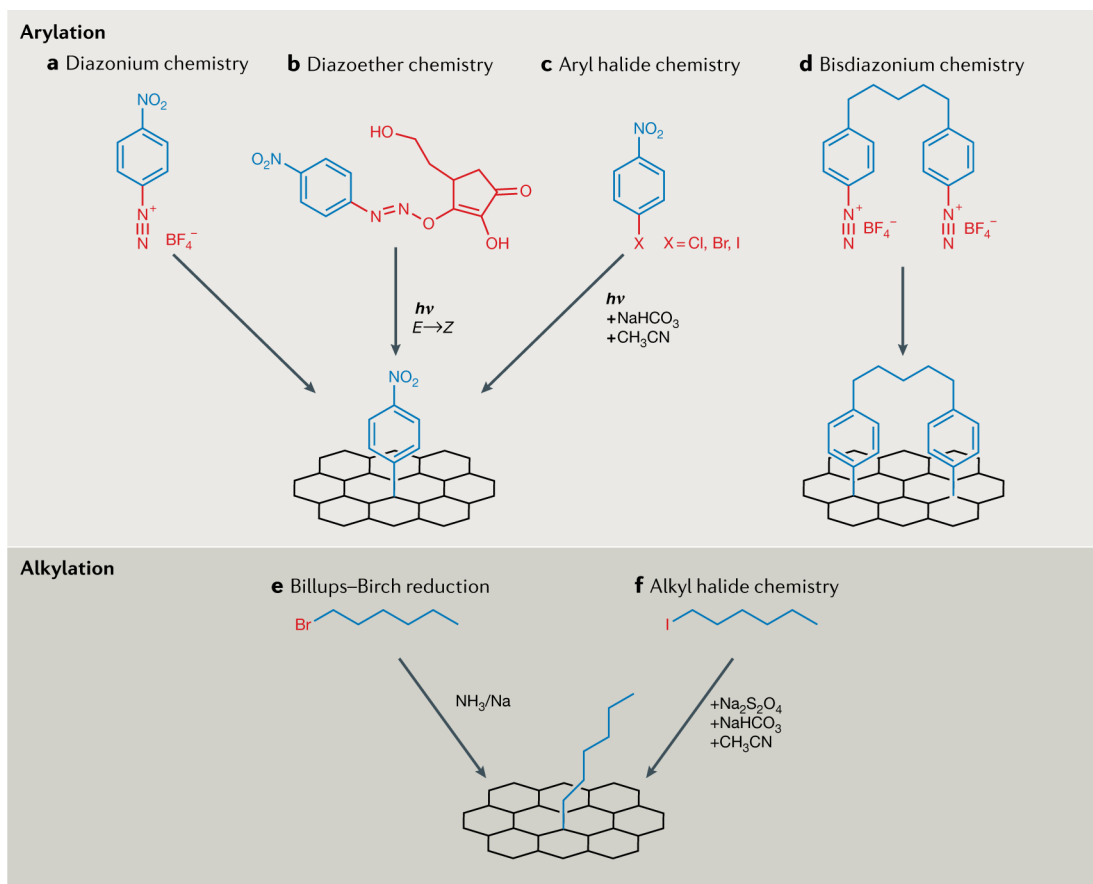


Fig. 5 | Chemistry of organic colour centres.

Various reactions have been developed to add aryl^{7,17,23,58} and alkyl^{8,99} organic colour centres to the surface of single-walled carbon nanotubes at controlled densities, converting sp^2 -hybridized carbon atoms of the host substrate to sp^3 . **a** | Arylation by reaction with a diazonium salt⁷. **b** | Arylation by reaction with diazoethers⁵⁸. **c** | Arylation by reaction with aryl halides¹⁷. **d** | Arylation by reaction with bisdiazonium salt²³. **e** | Alkylation by Billups–Birch reduction⁹⁹. **f** | Alkylation by reaction with an alkyl halide⁸. The choice of the substituent alkyl or aryl groups employed enables the nanotube electronic structure and resulting organic colour centre emission to be precisely tuned.

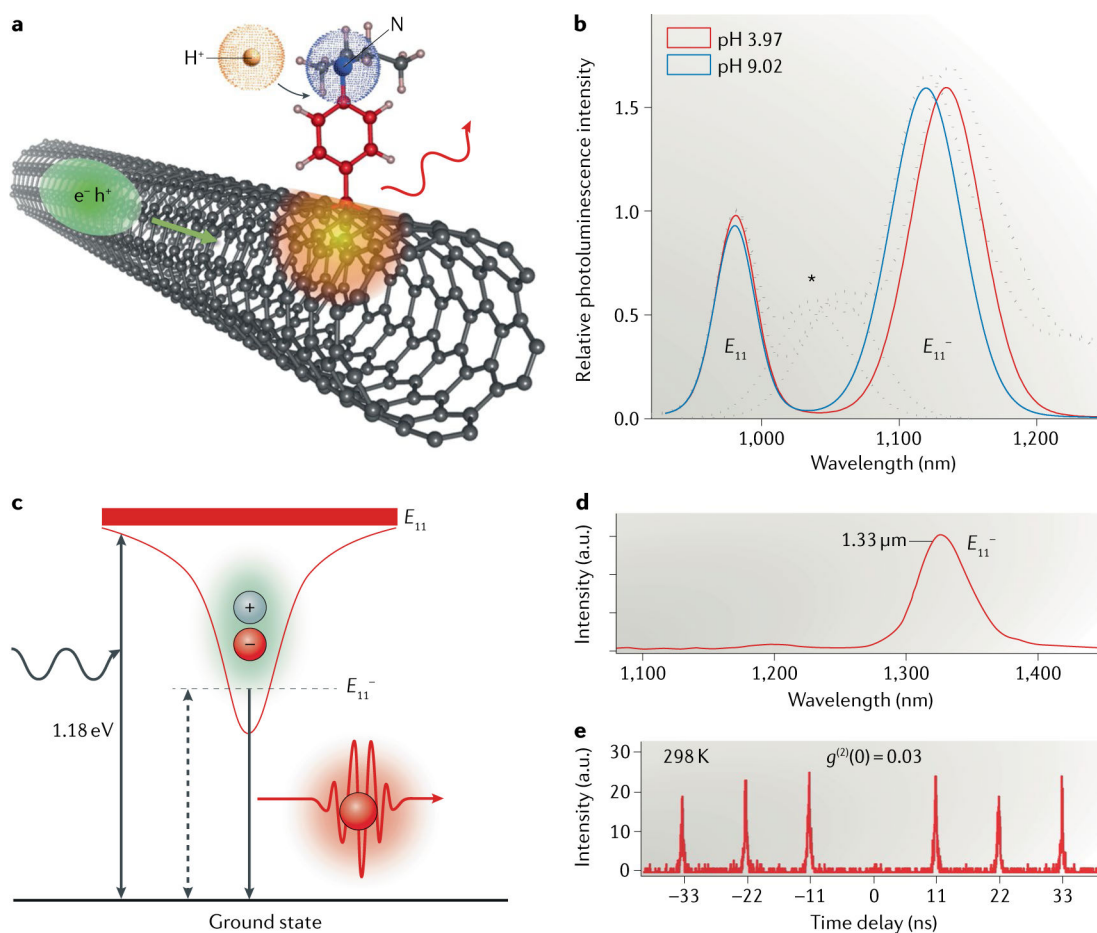


Fig. 6 |. Emergent applications of fluorescent organic colour centres.

a | Optical pH sensing in complex solutions within the biological window. A 4-*N,N*-diethylaminoaryl organic colour centre (OCC) on a (6,5)-single-walled carbon nanotube (SWCNT), which is protonated at low pH ($pK_a = 6.28$). **b** | The OCC photoluminescence shifts after changing the pH of a suspension of (6,5)-SWCNT- $C_6H_4N(C_2H_5)_2$. The asterisk denotes other nanotube chiralities present in the suspension. **c** | Radiative decay of OCC-trapped excitons produces single photons. The dashed lines represent the measured data, and solid lines represent isolated E_{11} and E_{11}^- peaks from spectral fitting. **d,e** | The photoluminescence spectrum (part **d**) and second-order time correlation (part **e**) of OCC photoluminescence in (7,5)-SWCNT- $C_6H_4OCH_3$ showing high-purity single-photon emission in the shortwave IR at room temperature. a.u., atomic units. Parts **a** and **b** are adapted with permission from REF.¹², ACS. Parts **c–e** are reproduced from REF.⁹, Springer Nature Limited.

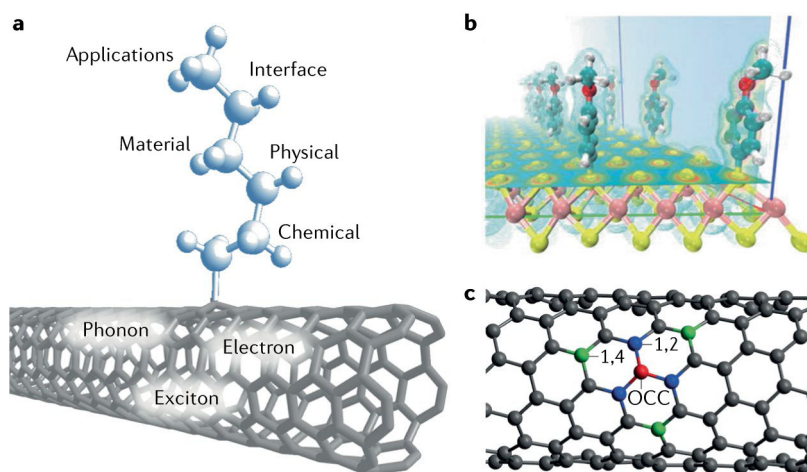


Fig. 7 | Opportunities and challenges for organic colour centres.

a | Organic colour centres (OCCs) provide a molecular site for studying the coupling of electrons, excitons, phonons and spin in low-dimensional materials, which are largely unexplored. **b** | Two-dimensional materials such as MoS_2 may function as interesting substrates for OCCs, in which the attachment of various organic groups to the crystal substrate could potentially produce new fluorescent emissions with controllable intensity and wavelength. **c** | OCCs break the symmetry of extended solids, posing significant challenges to theory in predicting the relative bonding sites, as highlighted by the many possible atomic configurations, including 1,2 sites (blue) and 1,4 sites (green), and describing the excited states. Part **b** is adapted with permission from REF.⁵⁶, ACS.

Table 1 | A comparison of organic colour centres with several state-of-the-art quantum systems

Material	Host	Excitation range	Emission range	Single-photon purity at room temperature	Quantum yield	Molecularly tunable?
Nitrogen-vacancy centre	Diamond	575 nm	630–800 nm	93% ⁴⁹	70% ⁵⁰	No
InAs/GaAs quantum dot ¹⁸	–	~900 nm	~900 nm	99% (<10 K)	20–70%	No
Carbon antisite–vacancy pair ⁵⁵	4H-SiC	<700 nm	650–680 nm	90%	70%	No
Organic colour centre	Single-walled carbon nanotube	Visible–shortwave IR	Shortwave IR ²⁸	99% ⁹	~16% (ensemble) ⁷	Yes

Author Manuscript


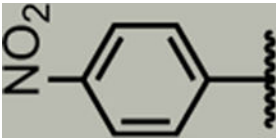
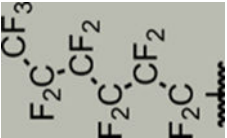
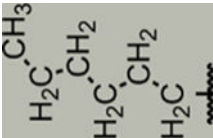
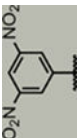
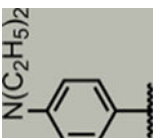
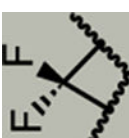
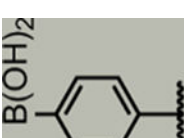
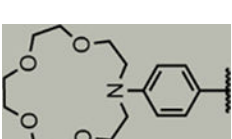

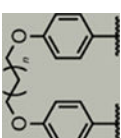

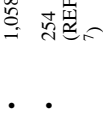
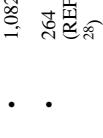
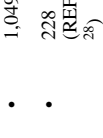
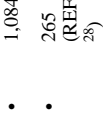
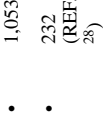
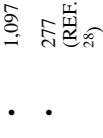





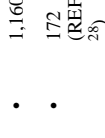
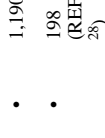
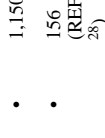
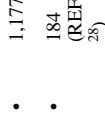

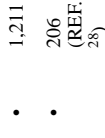





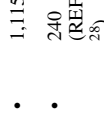
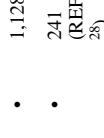
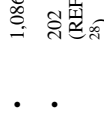
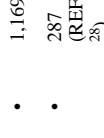






Author Manuscript

Author Manuscript

Author Manuscript

Table 2 |

Chemical tunability of organic colour centre photoluminescence in (n,m) -single-walled carbon nanotubes

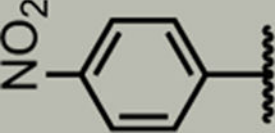

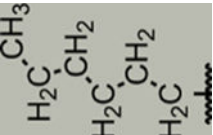
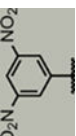
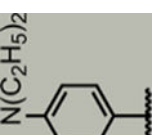

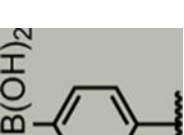
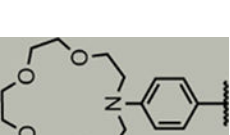
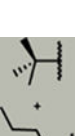
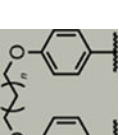
(5,4)												-	-	-	-	-	-
(6,4)												-	-	-	-	-	-
(7,3)												-	-	-	-	-	-
(9,1)												-	-	-	-	-	-

Author Manuscript

Author Manuscript

Author Manuscript

Author Manuscript

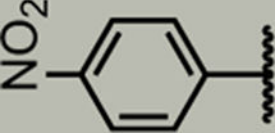

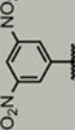
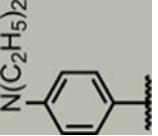
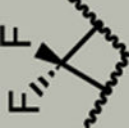
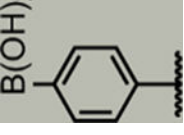
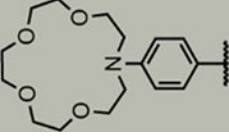

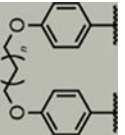
(6.5)										
	• 1,137	• 1,155	• 1,096	• 1,148	• 1,110	• 1,164	• 1,138 (REF. 24)	• 1,134	• 1,240	• 1,250
	• 181 (REF. 7)	• 190 (REF. 8)	• 133 (REF. 8)	• 192 (REF. 7)	• 175 (REF. 7)	• 200 (REF. 8)	• 164 (REF. 26)	• 271 (REF. 21)	• 267 (REF. 23)	
(8.3)	• 1,155	• 1,169	• 1,124	• 1,171	• 1,127	-	-	-	-	-
	• 241 (REF. 7)	• 238 (REF. 28)	• 195 (REF. 28)	• 237 (REF. 28)	• 200 (REF. 28)	-	-	-	-	-
(9.2)	• 1,300	-	-	-	-	-	-	-	-	-
	• 140 (REF. 7)	-	-	-	-	-	-	-	-	-
(7.5)	• 1,179	• 1,206	• 1,174	• 1,192	• 1,164	-	-	-	-	-
	• 170 (REF. 7)	• 173 (REF. 28)	• 151 (REF. 28)	• 162 (REF. 28)	• 136 (REF. 28)	-	-	-	-	-
(8.4)	• 1,263	• 1,284	• 1,228	• 1,282	• 1,242	-	-	-	-	-
	• 136 (REF. 7)	• 149 (REF. 28)	• 102 (REF. 28)	• 146 (REF. 28)	• 114 (REF. 28)	-	-	-	-	-

Author Manuscript

Author Manuscript

Author Manuscript

Author Manuscript

								
(11,0)	-	• 1,225 • 160 (REF. 28)	-	-	-	-	-	-
(7,6)	• 1,263 • 132 (REF. 7)	• 1,291 • 134 (REF. 28)	• 1,228 • 92 (REF. 28)	• 1,281 • 24 (REF. 28)	• 127 • 92 (REF. 28)	-	-	-
(9,4)	-	• 1,270 • 137 (REF. 28)	-	-	-	-	-	-
(11,1)	• 1,486 • 137 (REF. 28)	• 1,487 • 137 (REF. 28)	-	-	-	-	-	-
(10,3)	• 1,455 • 127 (REF. 28)	• 1,445 • 126 (REF. 28)	-	-	-	-	-	-

For each entry in the table, the top value is the E_{11}^- emission wavelength (in nanometres) and the bottom value is the energy shift from E_{11}^- (in millielectronvolts) for various nanotube chiralities and defects implanted using alkylation and arylation reactions and diazo compounds. Data obtained from REFS^{7,8,21,23,24,26,28}.

Author Manuscript

Author Manuscript

Author Manuscript

Author Manuscript